Modeling of Mn/ROAD Test Sections with the CRREL Mechanistic Pavement Design Procedure

Susan R. Bigl and Richard L. Berg

September 1996

Abstract: The U.S. Army Cold Regions Research and Engineering Laboratory is developing a mechanistic pavement design procedure for use in seasonal frost areas. The procedure was used to predict pavement performance of some test sections under construction at the Mn/ROAD facility. Simulations were conducted in three phases, investigating the effects on predictions of water table position, subgrade characteristics, asphalt model, and freeze season characteristics. The procedure predicted significantly different performance by the different test sections and highly variable results depending on the performance model applied. The simulated performance of the tests sections also was greatly affected by the subgrade conditions, e.g., density, soil moisture, and water table depth. In general, predictions for the full-depth asphalt sections indicate that they will not fail due to cracking, but two of the three criteria for subgrade rutting indicate failure before the five- or 10-year design life of the sections. Conventional sections are predicted not to fail due to subgrade rutting; however, sections including the more frost-susceptible bases in their design are predicted to fail due to asphalt cracking relatively early in their design life, and sections with non-frost-susceptible bases are predicted to fail towards the end of the design life.

Special Report 96-21

**US Army Corps
of Engineers**

Cold Regions Research &
Engineering Laboratory

Modeling of Mn/ROAD Test Sections with the CRREL Mechanistic Pavement Design Procedure

Susan R. Bigl and Richard L. Berg   September 1996

PREFACE

CONTENTS

ILLUSTRATIONS

TABLES

EXECUTIVE SUMMARY

The U.S. Army Cold Regions Research and Engineering Laboratory (CRREL) is developing a mechanistic pavement design procedure for use in seasonal frost areas. It consists of four computer programs that compute soil and pavement moisture and temperature conditions (FROST), resilient modulus and Poisson's ratio (TRANSFORM), stresses and strains in the pavement system (NELAPAV), and cumulative damage (CUMDAM). Damage predictions are based on several equations that employ horizontal strain at the base of an asphalt layer, vertical strain at the top of the subgrade, or horizontal stress at the base of a concrete layer. The procedure was used to predict pavement performance of some of the Mn/ROAD test sections. Laboratory tests on the Mn/ROAD materials (Bigl and Berg 1996a, Berg et al. 1996) provided the input parameters necessary for the modeling effort. Simulations were conducted in three phases, investigating the effects on predictions of water table position, subgrade characteristics, asphalt model, and freeze season characteristics.

Phase 1, conducted in the spring of 1991, included an initial simulation series that modeled temperatures from a year close to the mean freezing index. These boundary conditions were applied to eight flexible and three rigid sections. Phase 2, an effort in the summer of 1992, had two primary objectives. Phase 2A included three series modeling the eight flexible sections with the mean freeze season and changing the method employed to calculate the asphalt and subgrade moduli. Phase 2B investigated the variability in predictions when temperatures from freeze seasons with maximum and minimum freezing indices are applied to a single flexible section. Phase 3, an effort in the summer of 1993, expanded the investigation of the effects of freeze season characteristics. This series modeled 21 different freeze seasons applied to one full-depth and one conventional flexible section.

The procedure predicted significantly different performance by the different test sections and highly variable results depending on the performance model applied. The simulated performance of the test sections was also greatly affected by the subgrade conditions, e.g., density, soil moisture and water table depth. In general, predictions for the full-depth asphalt sections indicate that they will not fail due to cracking, but two of the three criteria for subgrade rutting indicate failure prior to the 5- or 10-year design life of the sections. Conventional sections are predicted not to fail due to subgrade rutting, but sections including the more frost-susceptible bases in their design are predicted to fail due to asphalt cracking relatively early in their design life, and sections with non-frost-susceptible bases are predicted to fail towards the end of their design life.

Modeling of Mn/ROAD Test Sections with the CRREL Mechanistic Pavement Design Procedure

SUSAN R. BIGL AND RICHARD L. BERG

INTRODUCTION

This is one of four reports related to the full-scale pavement test facility, Mn/ROAD, constructed by the Minnesota Department of Transportation (Mn/DOT) adjacent to Interstate 94 in Otsego, Wright County. One report describes the results of laboratory tests conducted to determine the physical and freeze-thaw related characteristics of the on-site subgrade and two of the pavement system materials used in the test sections (Bigl and Berg 1996a). Another report discusses resilient modulus tests conducted on the above materials (Berg et al. 1996). This report provides an initial description of the computer programs used in a mechanistic pavement design procedure under development by CRREL, and then describes a computer modeling effort that utilizes the results of the material testing program in the procedure to predict the performance of some Mn/ROAD test sections. The final report of the series summarizes information in the first three reports (Bigl and Berg 1996b).

The mechanistic pavement design procedure is being developed for use in seasonal frost areas and considers seasonal variations in pavement strength such as:

1. Large increases in base and subgrade strengths when frozen.
2. Loss of base and subgrade strengths during the spring when thawing and excess water weakens the layers.
3. Loss of asphaltic concrete strength during the summer months when asphalt moduli decrease with higher temperatures.

Availability of data from the Mn/ROAD facility will allow us to verify and refine various aspects of the model.

COMPUTER MODELS

The mechanistic design procedure consists of the four programs FROST, TRANSFORM, NELAPAV, and CUMDAM (Fig. 1). FROST predicts the amount of frost heave and thaw settlement of the pavement structure and conditions throughout the depth of the structure (temperature, water content, pore water pressure, ice content, density) at a given time increment. TRANSFORM uses the output from FROST as input and divides the pavement structure into "layers" based on moisture or temperature conditions. Each layer is then assigned a resilient modulus, Poisson's ratio and density value. NELAPAV, a nonlinear layered elastic program, calculates stresses, strains and deflections at specified locations within a pavement profile when a load is applied to the surface. CUMDAM calculates the incremental and cumulative damage the pavement undergoes using several available damage models. The behavior is normally modeled for a one-year period, with output on a daily basis. By assuming that the results from a single year will be repeated annually, the number of applications to failure is estimated.

FROST

FROST is a one-dimensional coupled heat flow and moisture flow model that computes frost heave and thaw settlement of a pavement or soil profile
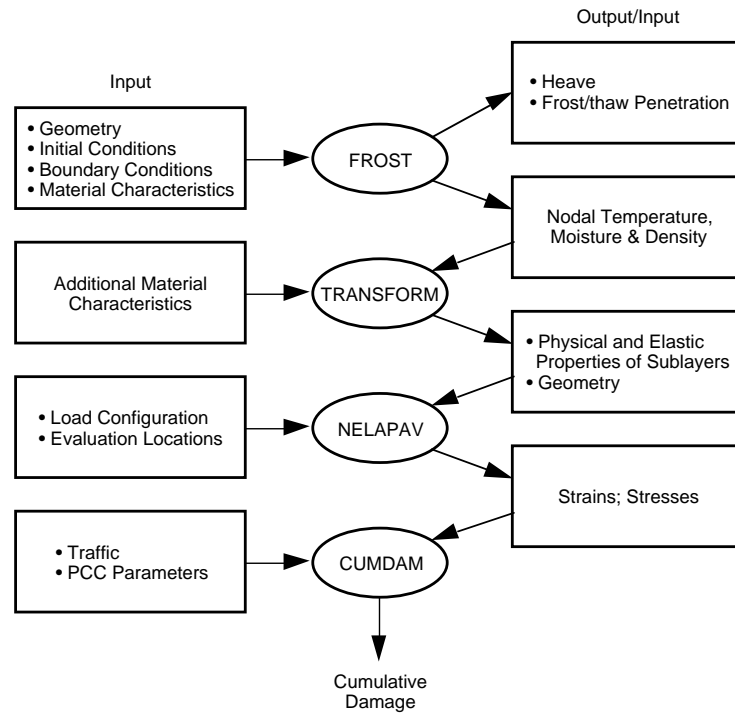
Figure 1. Flow chart of mechanistic design procedure.

with time. It also calculates temperature, moisture stress, water content, ice content, and density through the depth of the profile at each time increment. FROST was originally developed by Berg et al. (1980) in a cooperative study funded by the Corps of Engineers, the Federal Highway Administration, and the Federal Aviation Administration. Additional details beyond those described here are given in Guymon et al. (1993). The model assumes one-dimensional vertical heat and moisture flux and is based on a numerical solution technique termed the nodal domain integration method. The nodal domain integration method allows use of the same computer program to solve a problem by either the finite element method, the integrated finite difference method, or any other mass lumping numerical method. For this study, we chose to use the integrated finite difference computational method.

Figure 2 shows how FROST uses nodes, which are exact points, to divide the column of material into horizontal elements. Material properties are assigned to each element.

The program was developed for use on problems of seasonal freezing and thawing of non-plastic soils, and is based on the following primary assumptions, with additional assumptions reported in Guymon et al. (1993):

1. Darcy's law applies to moisture movement in both saturated and unsaturated conditions.
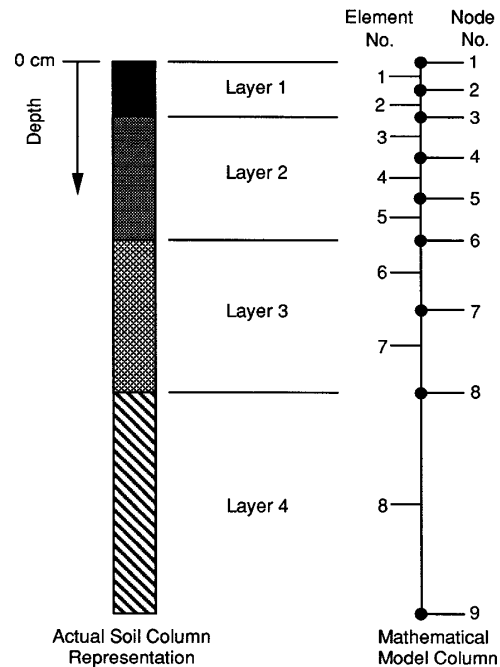
Figure 2. Example of pavement profile divided into finite elements.

2

2. The porous media are nondeformable as far as moisture flux is concerned; i.e., consolidation is negligible.
3. All processes are single valued; i.e., hysteresis is not present in relationships such as the soil water characteristic curve.
4. Water flux is primarily as liquid; i.e., vapor flux is negligible.

The governing equation used in FROST to describe soil moisture flow is derived by substituting the extended Darcy moisture-flow law into the one-dimensional continuity equation for an incompressible fluid flowing through porous media, i.e.,

$$\frac{\partial}{\partial x}\left[K_H \frac{\partial h}{\partial x}\right] = \frac{\partial \theta_u}{\partial t} + \frac{\rho_i}{\rho_w} \frac{\partial \theta_i}{\partial t} \tag{1}$$

where K_H = unsaturated hydraulic conductivity (permeability) (cm/hr)
h = total hydraulic head (cm water)
x = depth (cm)
θ_u = volumetric unfrozen water content (%)
ρ_i = density of ice (g/cm^3)
ρ_w = density of water (g/cm^3)
θ_i = volumetric ice content (%)
t = time (hr).

The total hydraulic head h equals the sum of the pore pressure head ($h_p = u/\rho_w$), where u is the pore water pressure, plus the elevation head ($h_e = -x$), where x is measured vertically downward. The ice sink term, $\rho_i \partial \theta_i / \rho_w \partial t$, exists only in freezing or thawing zones, and in these zones, eq 1 is coupled to the heat transport equation. The ice sink term assumes that θ_i is a continuous function of time.

In FROST, the soil water characteristics are represented using a relationship in the form of Gardner's (1958) equation:

$$\theta_u = \frac{\theta_o}{A_w \left|h_p\right|^\alpha + 1} \tag{2}$$

where θ_u = volumetric unfrozen water content (%)
θ_o = soil porosity (%)
h_p = pore pressure head (cm of water)
A_w = Gardner's multiplier for the moisture characteristics
α = Gardner's exponent for the moisture characteristics.

For each soil to be modeled, point values of θ_u and h_p are determined in a laboratory moisture retention test (Ingersoll 1981). Gardner's eq 2 is then fit to the data using a least squares approach to determine the best fit parameters A_w and α. Test results for the Mn/DOT materials are given in the first report of this series (Bigl and Berg 1996a).

Unsaturated hydraulic conductivity is also approximated in FROST using a Gardner's equation:

$$K_H = \frac{k_s}{A_K \left|h_p\right|^\beta + 1} \tag{3}$$

where K_H = unsaturated hydraulic conductivity (cm/hr)
k_s = saturated hydraulic conductivity (cm/hr)
h_p = pore pressure head (cm of water)
A_K = Gardner's multiplier for hydraulic conductivity
β = Gardner's exponent for hydraulic conductivity.

Point values of K_H and h_p for each soil are determined in the laboratory by an unsaturated hydraulic conductivity test (Ingersoll 1981), and, again, Gardner's eq 3 is fit to the data using a least squares approach to determine the best fit parameters A_K and β. See Bigl and Berg (1996a) for the test results on the Mn/ROAD materials.

Within the partially frozen zone, FROST reduces the unsaturated hydraulic conductivity using an empirical constant, termed the *E*-factor, combined with the ice content according to the following equation:

$$K_F = K_H\left(h_p\right) \times 10^{-E\theta_i} , E\theta_i \geq 0 \tag{4}$$

where K_F = the adjusted hydraulic conductivity in a partially frozen element (cm/hr)
E = an empirical constant, dimensionless
θ_i = volumetric ice content (%).

For this study, the *E*-factor was determined within the FROST program using an empirically derived equation based on the saturated hydraulic conductivity, k_s, in centimeters/hour:

$$E = \frac{5}{4}\left(k_s - 3\right)^2 + 6. \tag{5}$$

3

Frost heave is estimated from the total amount of ice segregation in the frozen zone by:

$$\theta_s = \theta_i - \left(\theta_o - \theta_n\right) \qquad (6)$$

where θ_s = volumetric segregated ice content (%)
  θ_o = porosity (%)
  θ_n = residual unfrozen water content (%).

If θ_s is greater than 0, ice segregation has occurred and the frost heave is computed by multiplying θ_s by the zone thickness. The θ_n parameter establishes the pore water stress at the freezing front for the solution of the moisture transport equation. In this study, θ_n was obtained by assuming a moisture tension of –800 cm of water and solving eq 2. The use of the –800 cm of water condition stems from that being the highest tension measured in various field studies. Thaw settlement from ice melting is the reverse process of that described above for ice segregation.

To conduct the calculations described above, FROST requires the following input for each material: 1) Gardner's coefficients for soil moisture characteristics, 2) Gardner's coefficients for hydraulic conductivity characteristics, 3) porosity and density of the soil, 4) thermal conductivity and volumetric heat capacity of the dry soil, and 5) the *E*-factor.

FROST also requires the following input for initial and boundary conditions: 1) element lengths, 2) upper- and lower-boundary pore water pressures, 3) upper- and lower-boundary temperatures, 4) initial temperature, pore pressure and ice content distributions with depth, 5) surcharge pressure, 6) freezing point depression and 7) modifier of the upper node during thaw.

In all cases, the pavement structure was simulated as a column with its upper boundary at the pavement surface and extending down to 400 cm (13.1 ft) using 99 elements. The length of elements within the expected zone of freezing (down to 110 cm or 3.6 ft) was about 2 cm (0.8 in.). These lengths were adjusted for individual cases to provide nodes positioned exactly at the depths where the interface between materials are located in the Mn/ROAD test sections. The deeper soil was modeled with element lengths of 4 cm between 110 and 230 cm (3.6–7.6 ft), 10 cm between 230 and 340 cm (7.6–11.2 ft), and

20 cm from 340 cm (11.2 ft) to 400 cm (13.1 ft).

The upper boundary pore water pressure was chosen to be computer-generated, as follows. When the profile is completely thawed and downward vertical drainage occurs, the surface pore water boundary condition is modeled by

$$\frac{\partial h}{\partial x} = 0 \qquad (7)$$

which means that the velocity flux across this boundary is zero. The upper-boundary condition is set to 0 cm of water when the upper-boundary temperature is above 0°C and frozen regions remain in the column. When the surface temperature is below 0°C, a specified constant upper-boundary pore pressure is used. To be consistent with previous studies, a value of –300 cm of water was used.

The lower-boundary pore pressure condition of FROST is set by specifying discrete pore water pressures that relate to the water table elevation at times when these conditions occur. At intermediate times, lower-boundary pore water pressures are linearly interpolated. For all the Mn/DOT cases, we set the lower boundary pore pressure to produce a constant water table depth throughout the simulation. We simulated the water table in each test section at the depth determined by field measurements to be representative of the on-site conditions. Where the measured water table varied through a test section, we conducted two simulations using the deepest and shallowest values.

Input for the upper boundary temperature condition consists of a set of specified times and temperatures that are implemented as step changes. Values were input in 24-hr increments using the mean daily air temperature. Conditions at Buffalo, Minnesota, were simulated, since this is the nearest station to the Mn/ROAD facility (16 km; 10 mi) with a reasonably long record of meteorological data. The time period simulated was 1 October 1959 to 14 November 1960. If the severity of a winter is judged by its air freezing index, the 1959–1960 winter is very near the average value for the 28-year period ending in 1987. The distribution of freezing indices at Buffalo during this time is shown in Figure 3. Starting the simulations on 1 October gave 30 days of computations before the first freeze event, allowing the
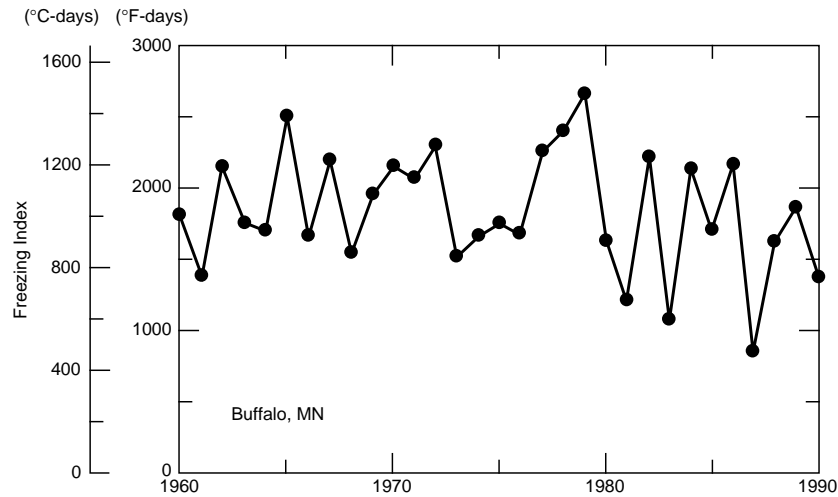
Figure 3. Distribution of seasonal freezing index with time at Buffalo, Minnesota.

model to stabilize and gradational moisture and temperature conditions to develop.

FROST adjusts the air temperature values to represent the soil surface temperatures using a procedure similar to the Corps of Engineers *n*-factor approach for seasonal freezing indices (U.S. Army 1966). An *n*-factor is defined as the ratio of the surface index to the air index, separately calculated for the full freeze and thaw season. In this study, 0.5 was used for the freezing *n*-factor (i.e., on days when the air temperature was ≤ 0°C), and 1.8 was used for the thawing *n*-factor.

Bottom boundary temperature conditions consist of a set of times and temperatures that are linearly interpolated at intermediate times. Three points were set during the simulations using estimated values of a reasonable ground temperature. The start and end temperatures are estimated to be 9.59°C (49.3°F), which is 3°C (5°F) higher than the mean annual air temperature 6.83°C (44.3°F). The third point was set so that a minimum value of 6.0°C (42.8°F) would occur at the end of the freeze season.

Initial conditions required to be set for the FROST program are temperature, moisture stress, and ice content. The initial temperature of all elements was estimated to be 5°F higher than the mean annual air temperature. For cases with water table depths less than 3 m (10 ft), the initial moisture tension/pressure was set at a gradient to produce a water table (i.e., pressure = 0) at the specified depth, increasing positively downwards at 1 cm water/1 cm depth. For simulations with

intermediate water table depths (3.6, 5.6 and 6.1 m; 12, 18, and 20 ft), the initial tension was set to –200 cm water (an estimate of optimum conditions) from the surface to the depth beneath which the tension from the theoretical gradient would increase positively. In simulations with the deepest in-situ water tables (13.7 and 15.2 m or 45 and 50 ft), we set a minimum bottom tension of –300 cm, with tensions decreasing from the bottom to 2 m (6.5 ft), and a constant tension of –200 cm water from 2 m (6.5 ft) to the surface. Initial volumetric ice content was set at 0.0% for all elements, since the simulations began prior to the start of the freeze season.

Surcharge (overburden) pressure is a constant value to simulate the pressure acting on the top node of the modeled column. In a case where only soil beneath a pavement surface is being modeled, this overburden should simulate the pressure of the pavement on the soil. For the Mn/ROAD test section simulations, the pavement properties were included in the modeled column, so the overburden pressure was set at zero.

The freezing point depression is a constant value that represents the temperature at which in-situ soil water freezes. This was set in all cases to be 0°C.

A modifier is included that adjusts the overburden pressure acting on the upper node during thaw periods. This value can be set between 0.0, to represent old, cracked pavements, and 1.0, to represent brand new pavements. We used 1.0 for the Mn/ROAD cases.

5

Standard procedures of FROST calculations were selected as follows. The fully implicit method was used for the moisture time domain solution, and the Crank-Nicolson method for the heat transfer time domain solution. Simulations were run with a time step of 0.2 hours, which is the time at which boundary conditions are adjusted; updates of the thermal and hydraulic properties were set to occur once per hour.

FROST produces what can be a very large output file. The first part of the file is a listing of the initial profile conditions, including all the input material properties. The next section is an incremental (usually daily) listing of the conditions generated for each node, including temperature, pore water pressure, water content, ice content, density, and porosity. The final section of the output file is a summary of the predicted frost heave and frost/thaw penetration data.

TRANSFORM

TRANSFORM was developed at CRREL by Chamberlain et al. (in prep.) and was modified extensively by Wendy Allen and Gregor Fellors, both of CRREL, for this study. The TRANSFORM program uses FROST daily output files as input and produces files of layered pavement systems where each layer is assigned a resilient modulus, Poisson's ratio, density and thickness. Output files from TRANSFORM are in the format to be used as input files to NELAPAV, the layered elastic program used to compute stresses and strains in the pavement system. NELAPAV requires a single file containing both load and structural data for each day of the simulation.

TRANSFORM first reads from a separate file a series of material type identifiers and their associated parameters needed for calculating the moduli of the materials in the frozen and thawed condition (see below). Then, TRANSFORM reviews the initial part of the FROST output file to determine the material type identifier for each element.

From the incremental (daily) listings of the FROST output file, TRANSFORM next reads the following conditions for each element: temperature, water content, ice content, material density, and porosity. A modulus value is then calculated for each element.

Moduli of surface paving materials were calculated as follows. PCC concrete had the modulus

set at a constant value of 3.4×10^7 kPa (5,000,000 lb/in.^{2}). In the initial two simulation series, the resilient modulus, M_r, of asphalt concrete layers were calculated by the equation (Schmidt 1975):

$$M_r(\text{lb/in.}^2) = 10^{(6.285 - 1.931 \times 10^{-2} T}$$
$$-3.280 \times 10^{-4} T^2 - 1.888 \times 10^{-5} T^3$$
$$+1.175 \times 10^{-7} T^4 + 1.502 \times 10^{-8} T^5$$
$$-2.022 \times 10^{-10} T^6) \qquad (8)$$

where T is the temperature of the element (°C). For pavement temperatures greater than 50°C, the asphalt modulus was set to 1.7×10^5 kPa (25,000 lb/in.^{2}); for temperatures less than –29°C, it was set to 3.3×10^7 kPa (4,840,000 lb/in.^{2}). In a third series of simulations, a second model was used for predicting asphalt moduli when the temperature was above 1°C (Ullidtz 1987):

$$M_r (\text{lb/in.}^2) = [15,000$$
$$-7900 \log (T)] \times 145.04. \qquad (9)$$

At below 1°C, the Schmidt (1975) relationship was used. Predictions of the two asphalt models are compared in Figure 4.

In the layers that represent an unstabilized base course, subbase or subgrade material, TRANSFORM calculates the modulus using regression equations developed from results of laboratory resilient modulus testing conducted on frozen and thawed soil samples (Berg et al. 1996). Each soil element is first classified using the criteria in Table 1 to determine which type of modulus equation is appropriate. The modulus is then calculated using one of the equations shown in general form in Table 2. The equations relate the frozen resilient modulus to temperature (through unfrozen water content), and the unfrozen resilient modulus to degree of saturation, stress condition, and to density for the class 6 special base course and the 1206 subgrade. The specific parameters for the Mn/ROAD materials will be discussed in a later section.

The following parameters, which are specific to each material, are used in the regression equations (Table 2): 1) FC1 and FC2, regression coefficients for the resilient modulus in the frozen condition, 2) TC1, TC2, TC3, and TC4, regres-
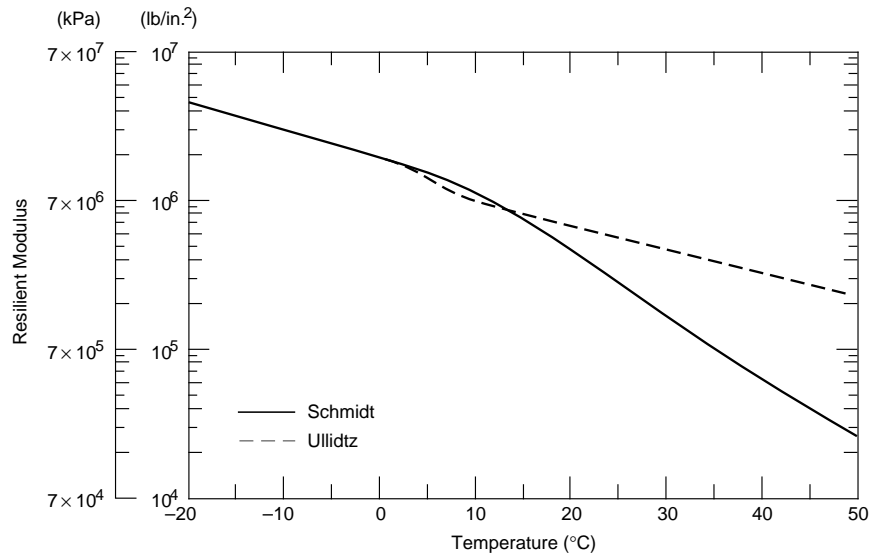
Figure 4. Comparison of predicted values from the Schmidt and Ullidtz asphalt modulus equations.

Table 1. Classification of soil for corresponding modulus equation.

Classification	Definition
1	Frozen: the ice content is greater than or equal to 0.005, the temperature not equal to 0°C, and the pore pressure less than 0.
2	Partially thawed: the ice content is greater than or equal to 0.005 and the pore pressure is greater than or equal to 0.
3	Thawed, with negative pore pressure: the ice content is less than 0.005 and the pore pressure is less than 0.
4	Thawed, with positive pore pressure: the ice content is less than 0.005 and the pore pressure is greater than 0.
5	Recently frozen layer: the temperature is less than 0°C and was recently thawed. This layer retains its modulus prior to freezing until the frozen equation predicts a higher modulus or until the temperature rises.
6	Recovering thawed layer: for 120 days subsequent to having been frozen, a thawed layer has its modulus reduced according to a ratio that diminishes over time.

sion coefficients for the resilient modulus in the thawed condition, 3) $f(\sigma)_m$, an approximation of the mean stress condition, and 4) α and β, unfrozen water content constants.

Several forms of the unfrozen water content function were investigated for predicting the frozen moduli of the Mn/ROAD materials, as reported in Berg et al. (1996). The form used for the Phase 1 simulation series of this study is the normalized gravimetric unfrozen water content, calculated as shown in Table 2. A second, normalized volumetric form of the unfrozen water content function was used in Phases 2 and 3 simulation

series. It is calculated by multiplying the gravimetric unfrozen water content by the dry density in Mg/m^3.

TRANSFORM uses an approximation of the $f(\sigma)$ stress term in its equations to predict moduli of unfrozen soils. Since this term is constant for each soil, the unfrozen moduli calculated by TRANSFORM are not dependent on stress. The approximation used was the mean stress condition applied during the laboratory resilient modulus testing.

Because some materials have a significant discontinuity between the minimum frozen and

7

Table 2. General form of resilient modulus (M_r) equations used in TRANSFORM.

Condition	Equation
Frozen	$M_r(\text{lb/in.}^2) = FC1\, f(w_{u-g})^{FC2}$
Partially thawed	$M_r(\text{lb/in.}^2) = TC1(100)^{TC3} f(\gamma)^{TC4} f(\sigma)_m^{TC2}$
Thawed, negative pore pressure	$M_r(\text{lb/in.}^2) = TC1\, f(S)^{TC3} f(\gamma)^{TC4} f(\sigma)_m^{TC2}$
Thawed, positive pore pressure	$M_r(\text{lb/in.}^2) = TC1(100)^{TC3} f(\gamma)^{TC4} f(\sigma)_m^{TC2}$

Notes:

$FC1, FC2$ = regression coefficients for the frozen condition

$f(w_{u-g})$ = w_{u-g}/w_o

w_{u-g} = grav. unfrozen water content (decimal) = $\dfrac{\alpha}{100}\left|\dfrac{T}{T_0}\right|^{\beta}$

w_o = unit water content (1.0)

α, β = unfrozen water content constants

T = temperature, °C

T_0 = 1.0°C

$TC1 - TC4$ = regression coefficients for the thawed condition

$f(S)$ = S/S_o

S = degree of saturation (%)

S_o = 1.0 %

$f(\gamma)$ = γ_d/γ_o

γ_d = dry density (Mg/m^3)

γ_o = 1.0 Mg/m^3

σ = stress (lb/in.^{2})

$f(\sigma)_m$ = a mean value of either $f_1(\sigma) = J_1/\sigma_o$

or $f_2(\sigma)$ = $(J_2/\tau_{oct})/\sigma_o$

or $f_3(\sigma)$ = τ_{oct}/σ_o

σ_o = 1.0 lb/in.^{2}

J_1 = bulk stress (lb/in.^{2}) = $3\sigma_3 + \sigma_d$

J_2 = 2nd stress invariant (lb/in.^{2}) = $3\sigma_3^2 + 2\,\sigma_3\sigma_d$

τ_{oct} = octahedral shear stress (lb/in.^{2}) $(\sqrt{2}/3)\,\sigma_d$

thawed predicted moduli, algorithms were added to TRANSFORM for providing a smoother transition in calculated moduli between the frozen and thawed condition. When the soil goes from an unfrozen to a frozen state, the modulus is held constant at its unfrozen value until either of two changes occur: 1) the soil becomes cold enough that the modulus as calculated by the frozen equation exceeds the pre-frozen modulus, or 2) the soil warms. When the soil warms, the modulus is set at the value calculated by the frozen equation and continues to follow the frozen curve until the soil is completely thawed. After complete thawing, the soil undergoes a 120-day "recovery period." During this time, the modulus value increases according to a power relationship with about one-half of the recovery taking place in the first 25 days about 75% recovery in 75 days and 100% recovery in 120 days.

After calculating the predicted modulus of an element, TRANSFORM also assigns it a Poisson's ratio using the criteria shown in Table 3.

After a modulus value has been assigned to all elements from a particular time step, adjacent ele-

Table 3. Poisson's ratio for the material layers.

Poisson's ratio	Condition
Asphalt	
0.30	Layer temperature is less than –2.0°C
0.35	Layer temperature is greater than or equal to –2.0°C and less than or equal to 1°C
0.40	Layer temperature is greater than 1°C and less than or equal to 8°C
0.45	Layer temperature is greater than 8°C
Concrete	
0.15	Constant for all conditions
Soil	
0.33	Thawed, volumetric ice content is less than 0.005
0.35	Frozen, volumetric ice content is greater than or equal to 0.005

ments within the same material type are combined into a single layer if the modulus of the deeper element is less than ±20% different from the modulus of the upper sublayer. A "weighted average" modulus of the two elements is then determined, with the weighting based on their relative lengths. The modulus of the next lower finite element is then compared with the modulus of the upper element. The checking and combining process continues until an element modulus is outside of the 20% limitation or if a layer of a different material or a different frozen/unfrozen state is encountered. In this manner, a particular material layer in the pavement profile may be divided into several sublayers. During the process of combining elements with similar modulus values, the thickness of each sublayer is also determined, as well as a weighted average of its other properties such as temperature, density and Poisson's ratio.

Typically, the pavement profile that was divided into 99 finite elements for the FROST program is combined by TRANSFORM into 5 to 20 sublayers with similar resilient modulus values. During the winter and spring a larger number of sublayers is more prevalent than in the summer months. TRANSFORM creates an additional "infinite" layer beneath the modeled column for passing to NELAPAV, which has its properties set the same as those for the bottom modeled sublayer.

Additional items must be input to (or generated from) TRANSFORM in order for it to create input files for NELAPAV. They include 1) loading information such as the total load on a specified loaded radius, or load pressure, 2) location and depth information related to the points where the stresses and strains are to be computed, and 3) a model number telling NELAPAV which form of the modulus equation to use for each material.

In the program, a 4082-kg (9000-lb) load was applied to a radius of 15.0 cm (5.91 in.), which approximates the area of a standard set of dual wheels or a falling weight deflectometer (FWD) testing plate. In all cases, stresses and strains were computed beneath the center of the load. For flexible pavements, the stress state at two points were analyzed: at the bottom of the pavement layer, and at the top of the subgrade. For rigid pavements, stress was computed only at the bottom of the pavement. In all cases the point of computation was 0.01 in. from the interface between materials.

NELAPAV

NELAPAV is an acronym for **N**onlinear **E**lastic **L**ayer **A**nalysis for **PAV**ements. It computes stresses, strains, and displacements at any point in an n-layered pavement system. The mainframe computer version of the program was developed by Lynne Irwin of Cornell University and Gregor Fellers of CRREL in 1980. The microcomputer version was developed by Irwin and Daniel Speck at Cornell University in 1984 and 1985 (Irwin and Speck 1986). The program is an adaptation of the Chevron Layered Elastic Systems program (CHEVLAY).

Irwin and Speck (1986) describe the computational approach used by NELAPAV and define the following terms. The term *state* of a point in a

9

layered system is used to refer to the set of stresses, strains, and displacements occurring at that point for a particular loading condition. A set of layer moduli $(M_{r1},...,M_{rn})$ is said to be *compatible at radius r* with a given set of non-linear models $(f_1,...,f_n)$ if each M_r agrees (within a specified tolerance) with the modulus determined by the model f_i evaluated at the middepth of layer i and at radius r.

The fundamental assumption of NELAPAV may be stated as follows: "The state of a point $p = (r,z)$ in a layered system is primarily determined by the modulus of elasticity of each of the layers in the system at the radius, r, of the point." Once this assumption has been made, the state of any point in the layered system may be determined by computing a set of compatible moduli at the radius of the point and then evaluating the resulting layered system at the point, holding the moduli constant.

NELAPAV operates as a "front-end" to CHEVLAY in that it calls the basic CHEVLAY
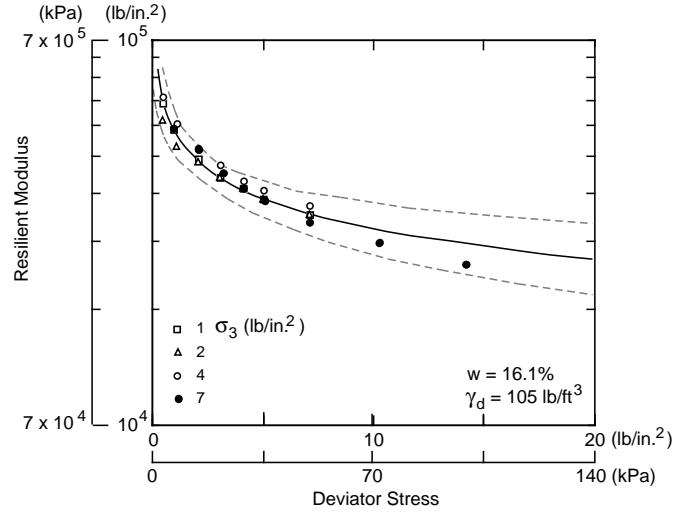
Figure 5. Stress dependence of resilient modulus in 1206 clay subgrade material (from Berg et al. 1996).

routines iteratively in order to come up with a set of compatible moduli for the layered system at the radius of each of the desired calculation points. The tolerances for compatibility used in this study

Table 4. Models currently available in NELAPAV (from Yang 1988).

Model no.	Name	Specification
0	Linear	$M_r = \text{constant}$
1	Bulk stress	$M_r = k_1 \theta^{k_2}$
2	Deviator stress	$M_r = \begin{cases} k_2 + k_3(k_1 - \sigma_d) & \sigma_d < k_1 \\ k_2 + k_4(\sigma_d - k_1) & \sigma_d \geq k_1 \end{cases}$
3	Second stress invariant	$M_r = k_1 (J_2 / \tau_{oct})^{k_2}$
4	Octahedral shear stress	$M_r = k_1 \tau_{oct}^{k_2}$
5	Vertical stress	$M_r = k_1 \sigma_v^{k_2}$
6	Major principal stress	$M_r = k_1 \sigma_1^{k_2}$
7	First stress invariant octahedral shear stress and anisotropic consolidation ratio	$M_r = k_1 (J_{10}^2 + J_{1p}^2)^{k_2} (1 + \tau_{oct})^{k_3} k_c^{k_4}$

Notes:

θ = bulk stress
k_1, k_2, k_3, k_4 = constants
σ_d = deviator stress
σ_v = vertical stress
σ_1 = major principal stress
J_{10} = first stress invariant due to overburden only
J_{1p} = first stress invariant due to overburden and load
k_c = anisotropic consolidation ratio

were a 2.0% maximum change in M_r from one iteration to the next and a total of 10 iterations.

NELAPAV allows the use of nonlinear (i.e., stress-dependent) modulus values in the analysis. Modulus values for thawing and unfrozen fine-grained soils are highly nonlinear as illustrated in Figure 5. Table 4, from Yang (1988), illustrates the various types of linear and nonlinear models currently available for use in NELAPAV; however, models 2 and 7 are not currently incorporated in the rest of the CRREL design procedure. In the CRREL version of NELAPAV, model 1 has been changed to the semi-log form:

$$M_r = k_1 e^{(k_2 \theta)} \tag{10}$$

where k_1 and k_2 are constants and θ is bulk stress. For this study, we utilized models 0, 1, 3, and 4, the specifics of which will be described in a later section.

One shortcoming of NELAPAV is that it allows only one circular load to be applied at the surface. This is not a major problem in this analysis because we are dealing with roadway pavements rather than airport pavements, which experience much more complex tire configurations.

Table 5 is a brief listing of the information included in a NELAPAV input file (Irwin and Speck 1986). It may contain up to 25 layers, with the following values for each: model number (from Table 4), seed modulus, Poisson's ratio, total density, lateral earth pressure coefficient, thickness, and the constants required for the equations from Table 4.

NELAPAV requires a seed modulus to begin its predictions of modulus for the various material layers. The value used for the seed modulus is the resilient modulus calculated in and passed from TRANSFORM. The constants required for computations are also passed from TRANSFORM. The k_2 value is a constant assigned on the basis of material type. The k_1 constant varies with the moisture/density level of the layer, and is calculated by multiplying together all the nonstress terms in the predictive equation for the material (Table 2).

Table 5. Format of a NELAPAV input file (from Irwin and Speck 1986).

Subject	input parameters
Header	problem description
Units	input units
Load	load, pressure, load radius
Layered system	n
	$M_1\ E_1$ seed $\nu_1\ \gamma_1\ K_{0,1}\ h_1\ k_{1,1}\ k_{2,1}\ k_{3,1}\ k_{4,1}\ t_1$
	$M_2\ E_2$ seed $\nu_2\ \gamma_2\ K_{0,2}\ h_2\ k_{1,2}\ k_{2,2}\ k_{3,2}\ k_{4,2}\ t_2$
	.
	.
	.
	$M_n\ E_n$ seed $\nu_n\ \gamma_n\ K_{0,n}\ h_n\ k_{1,n}\ k_{2,n}\ k_{3,n}\ k_{4,n}\ t_n$
Tolerance	maximum iterations, tolerance
Calculation points	r_1, z_1
	r_2, z_2
	.
	.
	.
	r_m, z_m

Notes:
n = number of layers
Supplied for each layer
M = model number (see Table 4)
E seed = seed modulus (lb/in.^{2})
ν = Poisson's ratio
γ = density (lb/ft^3)
K_0 = lateral earth pressure coefficient
h = thickness (in.)
k_1..k_4 = constants to be used in models (see Table 4)
t = mean temperature (°C)
r_m, z_m = radius, depth at which to make calculations (in.)

During this study, K_0, the coefficient of lateral earth pressure, was assigned to the layers as follows: a value of 1.5 was used for paving materials and frozen soil; a value of 1.0 was used for all unfrozen soil layers. We now feel that this system is too simplified, and are modifying the section of TRANSFORM that assigns K_0.

For each layer, NELAPAV expects to receive a value for the total density, which is adjusted to a buoyed density below the water table. In this study, however, we used dry density instead of total density, and neglected to adjust to a buoyed density below the water table. A short sensitivity study, conducted when these problems were discovered,

Table 6. Cumulative damage models used.

A. Flexible Pavement Horizontal Strain Criteria

1) The Asphalt Institute (MS-1, 1982):

$$N_a = 18.4 \ C \ (4.325 \times 10^{-3}) \left| \varepsilon_t \right|^{-3.291} \left[E_a^{-0.854} \right]$$

where N_a = number of load applications to 45% cracking
  C = a function of the volume of the voids and the volume of asphalt, 10^z
  z = $4.84 \ [(V_b / V_v + V_b) - 0.69]$
  V_b = volume of the asphalt, percent (11%)
  V_v = volume of the voids, percent (5%)
  ε_t = tensile strain at the bottom of the asphalt layer, in./in.
  E_a = modulus of the asphalt layer, lb/in.^{2}

2) Witczak (1972) (i.e., Asphalt Institute MS-11):

$$N_a = ab^{q^d} (1 / \varepsilon_t)^c$$

where a = 1.86351×10^{-17}
  b = 1.01996
  c = 4.995
  d = 1.45
  q = pavement temperature, °F

3) The Corps of Engineers (U.S. Army 1988):

$$N_a = 10^{(2.68 - 5 \log |\varepsilon_t| - 2.66 \log E_a)}$$

4) Coetzee and Connor (1990):

$$N_a = a \ \varepsilon_t^b \ E_a^c$$

where when $E_a \geq 1,500,000$ lb/in.^{2}: a, b, c = 3.364×10^6, –7.370, –4.470
  and when $E_a < 1,500,000$ lb/in.^{2}: a, b, c = 6.565×10^6, –5.764, –3.640

B. Flexible Pavement Subgrade Strain Criteria

1) The Asphalt Institute (1982):

$$N_s = 10^{[1/m \ (\log l - \log \varepsilon_v)]}$$

where N_s = allowable traffic based on subgrade strain
  m = a constant (0.25)
  l = a constant (2.8×10^{-2})
  ε_v = vertical strain at the top of the subgrade, in./in.

2) The Corps of Engineers (U.S. Army 1987):

$$N_s = 10000 \ (A / \varepsilon_v)^B$$

where A = $0.000247 + 0.00245 \log E_s$
  B = $0.0658 \ E_s^{0.559}$
  E_s = subgrade resilient modulus, lb/in.^{2}

Table 6 (cont'd).

C. Rigid Pavement Horizontal Stress Criteria

1) The Corps of Engineers (U.S. 1990):

$$N_h = 10^{[(df - adon)/bdon]}$$

where:
N_h = allowable traffic based on horizontal stress
df = R_{con}/σ_h
R_{con} = flexural strength of the concrete, lb/in.^{2}
σ_h = horizontal stress at the base of the concrete, lb/in.^{2}
$adon$ = 0.2967 + 0.002267 SCI
$bdon$ = 0.3881 + 0.000039 SCI
SCI = surface condition index of the pavement when failed

showed that this did not significantly affect the resultant strain calculations.

The solution computed by NELAPAV is an approximation of the exact solution. In reality, the stress state changes from point to point. Therefore, the modulus of a nonlinear material varies both vertically and horizontally. While NELAPAV recomputes the set of compatible moduli to determine the states of points at different radii, it is bound by the assumption that the moduli are constant everywhere in the layers. An exact theory for nonlinear materials would allow the modulus to vary horizontally within the layer in accordance with the nonlinear model.

Output from NELAPAV is one file for each day. The files include: 1) a repeat of the input information, 2) compatible moduli of the layers resulting from calculations, and 3) stress conditions for all points specified. For this study, the points specified were located 0.01 in. above the bottom of the asphalt or PCC and 0.01 in. below the top of the subgrade.

CUMDAM

The program CUMDAM calculates cumulative damage to the pavement structure, and was developed at CRREL. No report has been prepared that discusses its function and operation. In general form, the procedure used for CUMDAM's calculations is the linear summation of cycle ratios, referred to as Miner's rule, which may be stated as:

$$\sum_{i=1}^{i} \frac{n_i}{N_i} = D \qquad (11)$$

where n_i = number of applications at strain level i
N_i = number of applications to cause failure at strain level i, based on damage model predictions
D = total cumulative damage.

In this relation, failure can occur when D equals or exceeds 1.0. Thus, for a section to last its design life, the value of D should not accumulate to 1.0 until the design period expires.

The value n_i relates to the design traffic, or applications, in 8165-kg (18,000-lb) equivalent standard axle loadings (ESALs). For the first two simulation series in this study, anticipated traffic was considered to be 2,815,000 ESALs during a 5-year period. Since our incrementation was on a daily basis, we applied this as a constant loading of 1542 ESALs per day. In the final simulation series the anticipated traffic was revised upwards to 3,300,00 ESALs over five years, applied at a rate of 1808 ESALs per day.

CUMDAM includes several damage models previously developed by others for determining N_i the number of applications to failure at a particular strain/stress condition (Table 6). Of the damage models for flexible pavements, four are based on horizontal strain at the bottom of the asphalt layer, and relate to damage effects that result in pavement cracking. These models were developed by the Asphalt Institute (1982), Witczak (1972), the Corps of Engineers (U.S. Army 1988), and Coetzee and Connor (1990). Three other damage models for flexible pavements are based on

the vertical strain at the top of the subgrade, and these relate to rutting damage in the pavement. They were developed by the Asphalt Institute (1982), the Federal Aviation Administration (Bush 1980), and the Corps of Engineers (U.S. Army 1987). For rigid pavements, CUMDAM uses the damage model developed by the Corps of Engineers (U.S. Army 1990), which is based on the horizontal stress at the base of the PCC.

The program assumes that all applications will affect the point being modeled. That is, the damage is not reduced according to a pass-to-coverage algorithm to simulate the lateral wander of the axle within the travel lane.

It is recognized that some of the equations are being applied outside of the original assumptions used in their development; however, they are representative of cumulative damage models currently available and are used for the initial analysis until more appropriate equations can be developed.

The CUMDAM program first reads the strain/stress conditions from the daily NELAPAV out-put files and calculates the allowable applications predicted by the various models under those conditions. It then divides the design applications by the allowable applications, producing a daily incremental damage value. The incremental values are summed to produce a cumulative damage value and these are printed to individual files for each model type. A file summarizing the daily strain and deflection information is also produced.

MN/ROAD PAVEMENT PERFORMANCE STUDIES

Performance predictions using the Mechanistic Pavement Design Procedure were conducted in three major efforts:

Phase 1, conducted in the spring of 1991, included an initial simulation series that modeled temperatures from a year close to the mean freezing index. These boundary conditions were applied to eight flexible and three rigid sections.

Table 7. Layer composition and thicknesses of pavement structure in test sections simulated.

Test Section	Layer 1		Layer 2		Layer 3	
	Comp*	Thick †	Comp	Thick	Comp	Thick
Flexible						
5-yr design						
F-1	AC	14.6 (5.75)	CL4	83.8 (33.0)		
F-2	AC	14.6 (5.75)	CL6	10.2 (4.0)	CL4	71.1 (28.0)
F-3	AC	14.6 (5.75)	CL5	10.2 (4.0)	CL3	83.8 (33.0)
F-4	AC	22.2 (8.75)				
10-yr design						
F-14	AC	27.3 (10.75)				
F-19	AC	19.7 (7.75)	CL3	71.1 (28.0)		
F-21	AC	19.7 (7.75)	CL5	58.4 (23.0)		
F-22	AC	19.7 (7.75)	CL6	45.7 (18.0)		
Rigid						
5-yr design						
R-5	PCC	19.7 (7.5)	CL4	7.6 (3.0)	CL3	68.5 (27.0)
R-6	PCC	19.7 (7.5)	CL4	12.7 (5.0)		
10-yr design						
R-11	PCC	24.1 (9.5)	CL5	12.7 (5.0)		

*Composition:
   AC—asphalt concrete; PCC—portland cement concrete; CL3—class 3 special;
   CL4—class 4 special; CL5—class 5 special; CL6—class 6 special
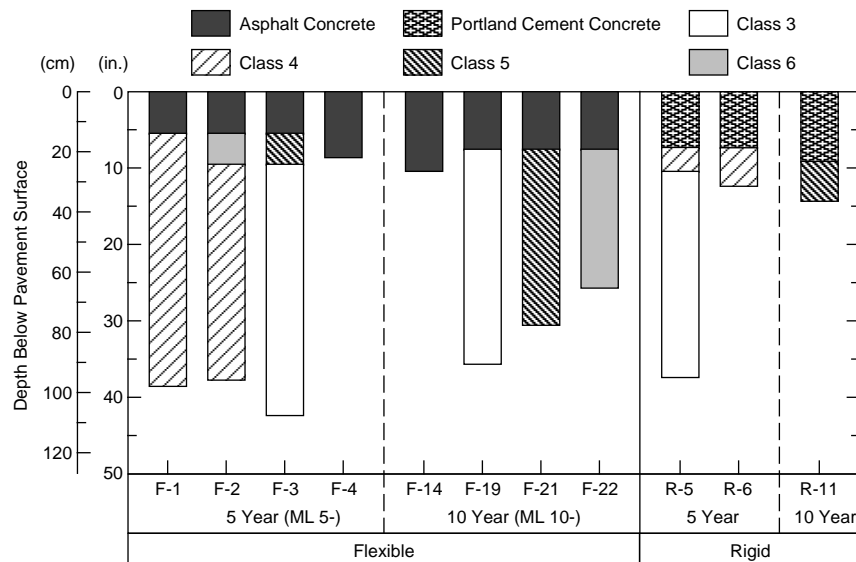†Thickness, cm (in.)

Figure 6. Pavement structure of Mn/ROAD test sections simulated.

Phase 2, an effort in the summer of 1992, had two primary objectives. Phase 2A included three series modeling the eight flexible sections with the mean freeze season and changing the method employed to calculate the asphalt and subgrade modulus. Phase 2B investigated the variability in predictions when temperatures from freeze seasons with maximum and minimum freezing indices are applied to a single flexible section.

Phase 3, an effort in the summer of 1993, expanded the investigation of the effects of freeze season characteristics. This series modeled 21 different freeze seasons applied to one full-depth and one conventional flexible section.

Phase 1

Pavement sections

The Mn/ROAD mainline facility has 23 test sections, including both flexible and rigid pavement systems, that are designed to fail after either 5 or 10 years. Included in the test matrix are pavement systems with various thicknesses and qualities of base and subbase materials. The base/subbase materials have a "special" Mn/DOT grading designation for the test facility and range from class 3, a well-graded sand, through classes 4 and 5, which have decreasing percentages of fines, to class 6, a well-graded gravel with sand. The subgrade at the site classifies as a sandy lean clay, a

CL in the Unified Soil Classification System and an A-6 in the AASHTO Classification System (Bigl and Berg 1996a). Of the four subgrade samples tested at CRREL, two exhibited high heaving in the frost susceptibility test, while the other two ranked as having a medium heave rate.

The mechanistic procedure was applied to 11 test sections, which were distributed among the designs as follows: four 5-year flexible, two 5-year rigid, four 10-year flexible, and one 10-year rigid. Figure 6 and Table 7 show the pavement structures of the test sections simulated. Seven of the test sections had variable water table depths along their lengths, and these were simulated at the two extreme water table positions. Table 8 lists the test sections and water table conditions simulated as well as the nomenclature used to denote the various cases. The case nomenclature includes the Mn/DOT test section number and the water table depth (in ft) preceded by a "*w*." For example, f1w9 refers to Mn/ROAD test section ML5-F-1 with a water table 2.7 m (9 ft) below the pavement surface and r11w6 refers to section ML10-R-11 with a water table 1.8 m (6 ft) below the pavement surface. All but one case involved the high-heaving subgrade (sample 1206) beneath the pavement structure. The final simulation included the lower-heaving subgrade (sample 1232) under the 5-year full-depth section (ML5-F4), termed case f4w6ss, or "second subgrade."

15

Table 8. Test sections and conditions analyzed.

Mn/ROAD test section	Water table Depth m (ft)	Simulation case	Other variations
FLEXIBLE			
5-year			
ML5-F-1	2.7 (9)	f1w9	
ML5-F-2	2.7 (9)	f2w9	
ML5-F-2	6.1 (20)	f2w20	
ML5-F-3	2.4 (8)	f3w8	
ML5-F-3	6.1 (20)	f3w20	
ML5-F-4	1.8 (6)	f4w6	
ML5-F-4	1.8 (6)	f4w6ld	Low density subgrade
ML5-F-4	1.8 (6)	f4w6ss	No. 1232 subgrade
10-year			
ML10-F-14	15.3 (50)	f14w50	
ML10-F-19	5.5 (18)	f19w18	
ML10-F-21	5.5 (18)	f21w18	
ML10-F-21	13.7 (45)	f21w45	
ML10-F-22	13.7 (45)	f22w45	
RIGID			
5-year			
ML5-R-5	1.8 (6)	r5w6	
ML5-R-5	3.7 (12)	r5w12	
ML5-R-6	1.2 (4)	r6w4	
ML5-R-6	3.7 (12)	r6w12	
10-year			
ML10-R-11	1.8 (6)	r11w6	
ML10-R-11	3.7 (12)	r11w12	

Material properties

Material properties input to the FROST program are shown in Table 9. The soil water characteristics are based on a best fit to the moisture retention test data using the Gardner's eq 2. Soil residual moisture contents were calculated using eq 2 with a pressure of –800 cm water. The soil permeability characteristics result from fitting the Gardner's eq 3 to unsaturated hydraulic conductivity test results.

As part of this study, Mn/DOT class 3 special, class 6 special, and two subgrade materials had been tested to determine the information for input to the model. Results of the soil characterization tests are given in Bigl and Berg (1996a). The class 4 special and class 5 special materials were not tested, so their behavior had to be approximated using data from previously tested materials that most closely matched their specified size gradations. A subbase from taxiway A at the Albany,

New York, airport most closely matched the class 4 special subbase specifications; dense-graded stone, which had been tested during a cooperative study in Winchendon, Massachusetts, most closely matched the class 5 special material. Results of the characterization tests of the substitute materials are also given in Bigl and Berg (1996a) and in Cole et al. (1986, 1987).

The densities of the Mn/ROAD materials, which had been characterized with compaction testing, were set at the optimum values. For the substitute materials, the densities were set at the values determined from in-place samples taken from the site. To demonstrate the influence of proper compaction, one simulation (case f4w6ld) involved setting the density of the 1206 subgrade to a reduced value less than optimum (1.69 Mg/m^3, 105.5 lb/ft^3). Optimum density was set at 1.89 Mg/m^3 (117.9 lb/ft^3), determined with a compactive effort of 2360 kJ/m^3 (55,000 ft-lb/ft^3).

Table 9. Material parameters input to FROST for Mn/ROAD test section simulations.

Parameter	Asphalt	(PCC) Concrete	Class 6	(DGS) Class 5	(TAS) Class 4	Class 3	(1206) Subgrade	(1232) Subgrade
Soil density (g/cm^3)	2.3	2.3	2.09	1.89	2.16	2.11	1.89	1.99
Specific heat of soil (cal/g °C)	0.2	0.2	0.2	0.2	0.2	0.2	0.2	0.2
Thermal cond. of soil (cal/cm hr °C)	17.5	17.5	17.0	17.0	17.0	17.0	17.0	17.0
Soil porosity (cm^3/cm^3)	0.14	0.14	0.331	0.337	0.206	0.251	0.374	0.320
Soil water characteristics: A_w	0.3090	0.3090	1.0001	0.4961	0.152	0.1735	0.00240	0.00226
α	0.3190	0.3190	0.4444	0.3660	0.269	0.3239	0.7134	0.6790
Residual water content (cm^3/cm^3)	0.039	0.039	0.01614	0.05008	0.10741	0.09994	0.2916	0.2638
Saturated hydraulic cond. (cm/hr)	2.10	1.05	6.0	5.54	2.8	4.5	0.14	0.0087
Permeability characteristics: A_k	0.0349	0.0349	3.723×10^{-8}	3.912	6.58×10^{-5}	1647.1	0.000571	0.001886
β	2.6450	2.6450	5.6733	1.3930	2.962	0.7207	2.6395	1.8129

Table 10. Modulus equations used for Mn/ROAD test section simulations.

A. Frozen condition

Material	Equation (M_r in lb/in.²)*	n	r^2	Std. error
Clay subgrade sample 1206 (565)				
Frozen	$M_r = 1,049 f(w_{u-g})^{-2.344}$	207	0.99	0.275
Frozen	$M_r = 1,052 f(w_{u-v})^{-2.929}$	207	0.99	0.262
Clay subgrade sample 1232 (566)				
Frozen	$M_r = 846 f(w_{u-g})^{-2.161}$	244	0.98	0.423
Frozen	$M_r = 848 f(w_{u-v})^{-2.633}$	244	0.98	0.394
Class 3 special "stockpile"				
Frozen	$M_r = 5,488 f(w_{u-g})^{-1.076}$	210	0.97	0.507
Frozen	$M_r = 5,542 f(w_{u-v})^{-1.249}$	186	0.97	0.467
Class 4 special (taxiway A subbase)				
Frozen	$M_r = 1,813 f(w_{u-g})^{-1.733}$	85	0.93	0.885
Frozen	$M_r = 1,652 f(w_{u-v})^{-2.813}$	69	0.91	0.916
Class 5 special (dense graded stone)				
Frozen	$M_r = 8,695 f(w_{u-g})^{-1.2814}$	28	0.95	0.511
Frozen	$M_r = 9,245 f(w_{u-v})^{-1.489}$	28	0.97	0.432
Class 6 special "stockpile"				
Frozen	$M_r = 19,427 f(w_{u-g})^{-0.795}$	260	0.98	0.338
Frozen	$M_r = 19,505 f(w_{u-v})^{-0.897}$	260	0.98	0.341

Notes:

n = number of test points

r^2 = coefficient of determination

M_r = resilient modulus

$f(S) = S/S_o$ σ = stress (lb/in.²)

S = degree of saturation (%) $f_1(\sigma) = J_1/\sigma_o$

S_o = 1.0 % $f_2(\sigma) = (J_2/\tau_{oct}/\sigma_o$

$f(\gamma) = \gamma_d/\gamma_o$ $f_3(\sigma) = \tau_{oct}/\sigma_o$

γ_d = dry density (Mg/m³) σ_o = 1.0 lb/in.²

γ_o = 1.0 Mg/m³ J_1 = bulk stress (lb/in.²)

$f(w_{u-g}) = w_{u-g}/w_o$ $J_1 = 3\sigma_3 + \sigma_d$

w_{u-g} = gravimetric unfrozen water content J_2 = 2nd stress invariant (lb/in.²)

w_o = unit water content (1.0) $J_2 = 3\sigma_3^2 + 2\sigma_3\sigma_d$

$f(w_{u-v}) = w_{u-v}/w_o$ τ_{oct} = octahedral shear stress (lb/in.²)

w_{u-v} = volumetric unfrozen water content $\tau_{oct} = (\sqrt{2}/3)\sigma_d$

*Output from equations can be converted to kilopascals by multiplying by 6.895.

Saturated hydraulic conductivities were set at the laboratory-determined value, except in the case of the 1206 clay subgrade. In that case, we multiplied the laboratory value by 10 to approximate the hydraulic behavior after formation of frost-induced shrinkage cracks.

The modulus equations used in TRANSFORM for the Phase 1 modeling are the normalized gravimetric form shown in Table 10a and the unfrozen form shown in Table 10b. The associated unfrozen water constants utilized in the frozen form of the equations are given in Table 11. Development

Table 10 (cont'd).

B. Unfrozen condition

Material	Equation (M_r in lb/in.²)*	n	r^2	Std. error
Clay subgrade sample 1206 (565)				
Never Frozen	$M_r = 1,597,000\, f(S)^{-2.63}\, f(\gamma)^{14.42}\, f_3(\sigma)^{-0.257}$	655	0.82	0.251
Clay subgrade sample 1232 (566)				
Never Frozen	$M_r = 1.518 \times 10^{30}\, f(S)^{-13.85}\, f_3(\sigma)^{-0.272}$	451	0.95	0.328
Class 3 special "stockpile"				
Thawed	$M_r = 283,300\, f(S)^{-1.003}\, f_2(\sigma)^{0.206}$	408	0.86	0.520
Class 4 special (taxiway A subbase)				
Thawed	$M_r = 8.946 \times 10^8\, f(S)^{-3.026}\, f_2(\sigma)^{0.292}$	149	0.86	0.168
Class 5 special (dense graded stone)				
Thawed	$M_r = 382,400\, f(S)^{-0.8759}\, f_2(\sigma)^{0.1640}$	64	0.77	0.164
Class 6 special "stockpile"				
Thawed	$M_r = 1,391\, f(S)^{-0.507}\, f(\gamma)^{4.04}\, f_1(\sigma)^{0.608}$	492	0.79	0.232
Thawed	$M_r = 5,257\, f(S)^{-0.486}\, f(\gamma)^{4.05}\, e^{\,0.0193 f_1(\sigma)}$	492	0.76	0.249

a. Frozen condition.　　　　*b. Thawed condition.*
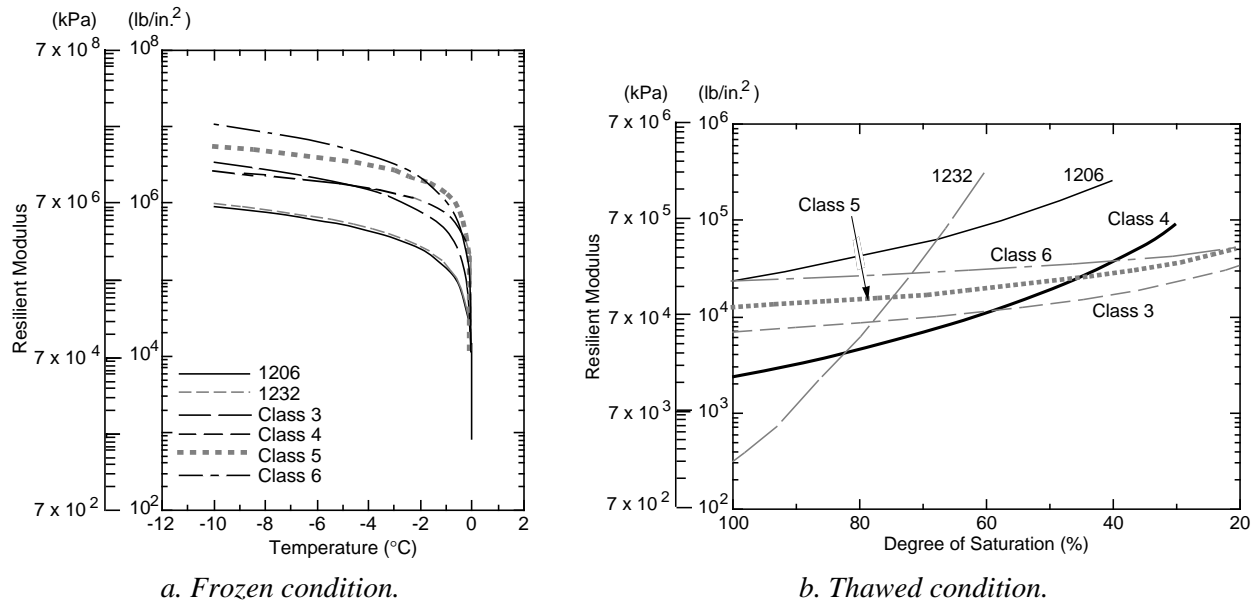
Figure 7. Predicted moduli of Mn/ROAD materials.

of these equations is discussed in Berg et al. (1996). Figure 7 shows the predicted moduli for the Mn/ROAD materials using mean values for stress and density, where applicable.

It should be noted that the thawed modulus equation used for class 6 special material is an exception to general form given in Table 2. In this case, we used a semi-log form (eq 10), rather than the log-log form, which eliminated problems that

occurred from negative stresses generated by the model.

It should also be noted that after the Phase 1 simulations were completed, we discovered that resilient modulus tests on the 1206 subgrade in the unfrozen condition were probably in error due to a miscalibrated testing system. As a result, the unfrozen subgrade moduli predicted in Phase 1 modeling are likely to be substantially higher than

Table 11. Constants for equations to determine gravimetric unfrozen moisture content, w_{u-g}.

Soil	Equation constants*	
	α	β
Subgrade		
1206	11.085	–0.274
1232	8.121	–0.303
Class 3 special		
stockpile	1.497	–0.709
Class 4 special		
Taxiway A	3.0	–0.25[†]
Class 5 special		
Dense stone	2.0	–0.40[†]
Class 6 special		
Stockpile	0.567	–1.115

* w_{u-g}, decimal form $= \dfrac{\alpha}{100}\left|\dfrac{T}{T_0}\right|^{\beta}$

[†] Values for these materials are estimated

exist in the field, resulting in less damage than would have been obtained with more reasonable moduli.

The model numbers for the program NELAPAV (Table 4) were set as follows. Model 0, the linear model, was used at all times for paving materials and for soils in the frozen state. With model 0, the seed modulus is accepted as the modulus of the material layer. Model numbers were assigned to unfrozen soils as follows: Model 1—class 6; Model 3—class 3 and class 4; Model 4—both clay subgrades.

In all of the cumulative damage studies on the flexible pavements, it was assumed that the pavement properties were constant from one pavement test section to another. Some of the test sections we simulated will have pavement properties different from others because of the experimental design of the paved surface. Some variations in the asphalt pavement properties could be considered in subsequent modeling efforts, but we maintained the same asphalt pavement properties in all of these simulations.

Results—flexible sections

Output from FROST for the 5-year full-depth simulation (f4w6) is shown in Figure 8. The top graph shows the daily mean air temperature for the period from 1 October 1959 to 14 November 1960. The center portion illustrates the predicted frost heave and the bottom graph contains the predicted frost and thaw penetration as functions of time. Frost output graphs for all the flexible cases are compiled in Appendix A. Table 12 contains maximum frost heave and maximum frost penetration depths for each of the cases simulated (Table 8). Simulations with shallower water table depths had greater amounts of heave and less frost penetration compared to simulations with a deeper water table location. Sections that included the substitute for the class 4 special subbase (taxiway A subbase) had higher amounts of heave than those with other combinations of subbase materials.
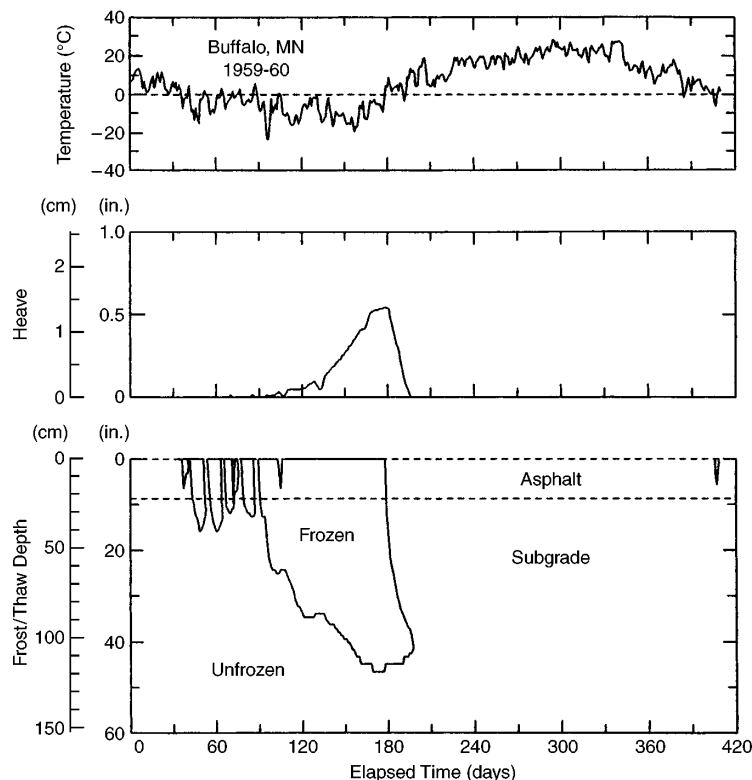

Figure 8. Example output from FROST for Mn/ROAD test section ML5-F4 with a 1.8-m (6-ft) water table. Simulation starts on 1 October.

20

Table 12. Maximum frost heave and frost penetration in modeled simulations

Cases	Frost heave cm (in.)	Frost penetration cm (in.)
5-YEAR		
Flexible		
f1w9	0.25 (0.10)	137.9 (54.3)
f2w9	1.19 (0.47)	121.9 (48.0)
f2w20	0.33 (0.13)	142.0 (55.9)
f3w8	0.08 (0.03)	134.1 (52.8)
f3w20	0.00	142.0 (55.9)
f4w6	1.37 (0.54)	118.1 (46.5)
f4w6 ld	1.32 (0.52)	118.1 (46.5)
f4w6 ss	0.03 (0.01)	137.9 (54.3)
Rigid		
r5w6	1.04 (0.41)	121.9 (48.0)
r5w12	0.00	137.9 (54.3)
r6w4	4.72 (1.86)	103.9 (40.9)
r6w12	0.00	134.1 (52.8)
10-YEAR		
Flexible		
f14w50	0.00	134.1 (52.8)
f19w18	0.00	142.0 (55.9)
f21w18	0.00	134.1 (52.8)
f21w45	0.00	134.1 (52.8)
f22w45	0.00	134.1 (52.8)
Rigid		
r11w6	1.42 (0.56)	118.1 (46.5)
r11w12	0.00	134.1 (52.8)

ld = low density (1.69 Mg/m^3 or 105.5 lb/ ft^3)
ss = second subgrade (1232)

Figure 9 presents the moduli being calculated by TRANSFORM and passed as seed moduli to NELAPAV for the f4w6 case. The plotted moduli are the minimum values for each day, with the subgrade (top) being located within 0.3 m (1 ft) of the asphalt and subgrade (bottom) being the rest of the modeled section (to 4.0 m or 13.1 ft). Note that the predicted asphalt moduli during the summer months are smaller than those of the subgrade, which results in high horizontal strains at the base of the asphalt layer during the summer months. In later simulations (Phase 2 and 3), we used other models to determine the asphalt modulus.

Figure 10 shows the deflection and strains computed by NELAPAV for the f4w6 case. The horizontal strain at the base of the asphalt is low through the winter with a few small peaks during short-term thaw periods, then exhibits high peaks during spring thaw and summer. It appears to be closely tied to the asphalt temperature/modulus during the spring thaw. The vertical strain at the top of the subgrade is also low during the winter with three sharp peaks during thaw events. The vertical strain also rises during spring and summer, closely tracking the pavement surface temperature. The deflection plotted is from the base of the asphalt, but is assumed to be similar to the surface deflection. It also shows peaks during midwinter thaws, and a maximum peak during the spring prior to drainage of excess moisture. Generally, deflections in the summer are greater than winter values.
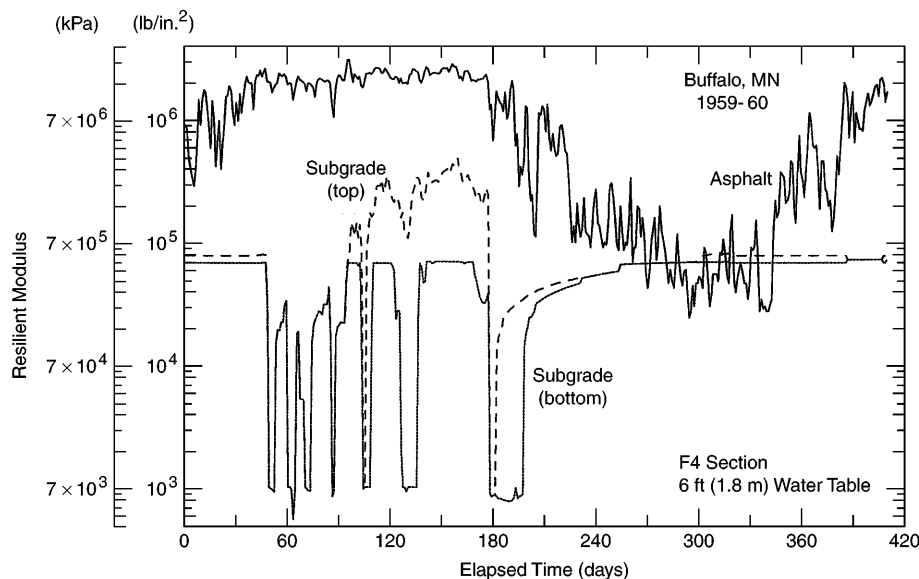

Figure 9. Seed moduli output by TRANSFORM for Mn/ROAD test section ML5-F4 with a 1.8-m (6-ft) water table. Subgrade (top) is within the upper 0.3 m (1 ft) of subgrade beneath the asphalt. Subgrade (bottom) is beneath that layer to the bottom of the modeled section.
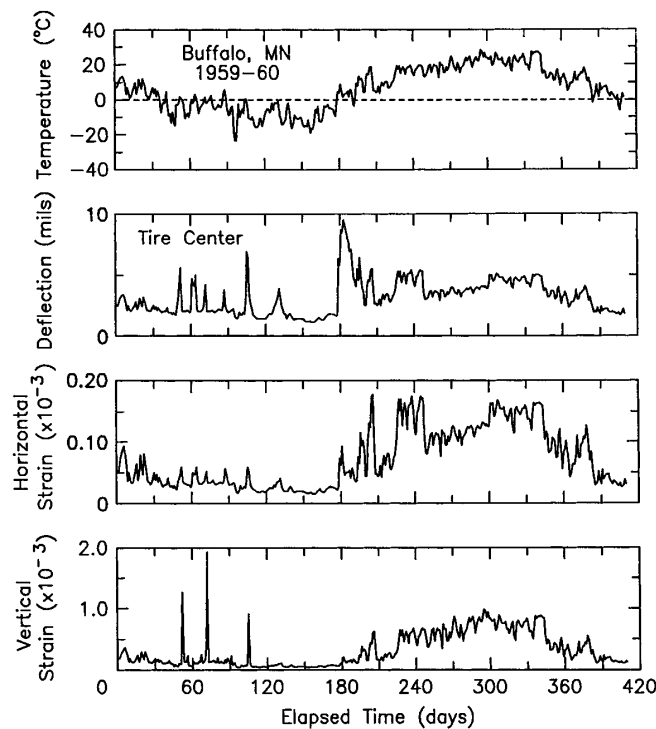
21

Figure 10. Deflection and strain calculated by NELAPAV for Mn/ROAD test section ML5-F4 with a 1.8-m (6-ft) water table. Horizontal strain is at the base of the pavement. Vertical strain is at the top of the subgrade.

Table 13 lists the applications to failure predicted from the 1-year simulation period applied to the flexible sections. The values listed in Table 13 were determined by taking the reciprocal of the one year (365-day) cumulative damage value produced by the CUMDAM program and multiplying by the number of applications received by the sections during that time period (562,830 per year). This application rate was based on an initial estimate that the traffic across the test sections would be 2,815,000 ESALs in 5 years, or 5,630,000 ESALs in 10 years. Note that the values listed in Table 15 are thousands of ESAL applications. Subsequent to conducting the Phase 1 series, a revised estimate is that the 5-year sections will receive 3,300,000 ESAL applications in five years, (i.e., are designed to fail after 3,300,000 ESAL applications); the 10-year sections will fail at 6,600,000 ESAL applications.

Individual values listed in Table 13 vary anywhere from very much below to very much above the failure values described. By comparing values horizontally across the table for any case, it can be seen that different models esti-

Table 13. Predicted applications to failure ($\times$ 1000) from Phase 1 simulation series of flexible pavement test sections.

| | Horizontal criteria | | | | Vertical criteria | | |
Cases	Asp. Inst. MS-1	Asp. Inst. MS-11	Corps of Engineers	Coetzee/ Connor	Asp. Inst. MS-1	Corps of Engineers	FAA
5-YEAR							
F1W9	86	498	88	4,380	136,942	5,653	11,879
F2W9	522	1,244	550	42,703	32,477	1,345	1,526
F2W20	722	1,534	764	66,450	155,909	8,226	9,855
F3W8	957	1,706	958	92,419	116,287	2,653	9,611
F3W20	1,068	1,801	1,055	105,202	222,462	7,889	20,632
F4W6	28,585	75,751	90,926	$>10^7$	3,715	15	152
F4W6ld	1,905	20,209	7,036	$>10^7$	165	$>10^7$	$>10^7$
F4W6ss	72	1,180	96	$>10^7$	$>10^7$	$>10^7$	$>10^7$
10-YEAR							
F14W50	103,272	485,198	605,194	$> 10^7$	8,602	10	251
F19W18	396	6,148	966	75,751	2,962,263	56,680	457,585
F21W18	3,394	30,456	12,751	2,010,107	562,830	84,382	42,478
F21W45	3,404	30,358	12,794	2,010,107	611,772	92,571	48,188
F22W45	7,614	57,315	31,147	8,040,429	73,190	22,415	3,388

Notes:
  ld = low density (1.69 Mg/m^3 or 105.5 lb/ft^3)
  ss = second subgrade (1232)
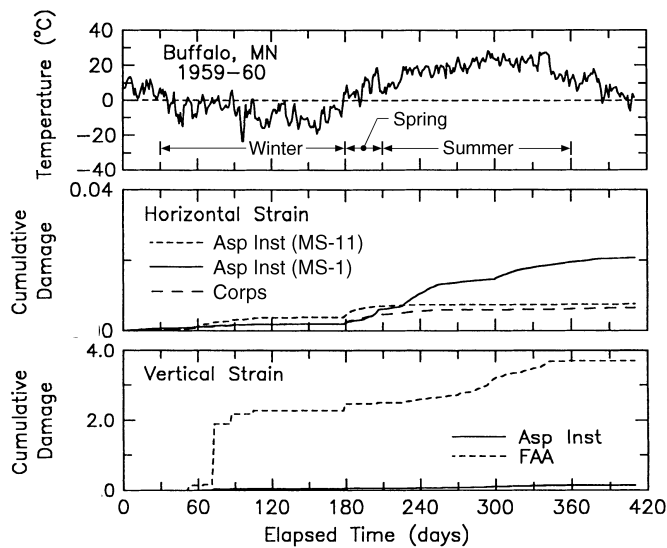 Traffic simulated at rate of 562,830 ESAL applications/yr

22

Figure 11. Cumulative damage for case f4w6 with optimum density 1206 subgrade.
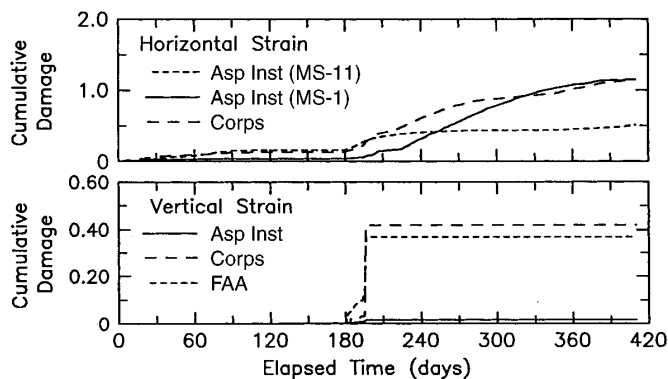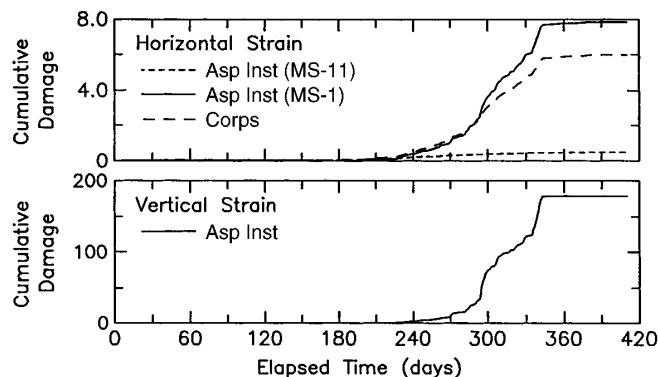

Figure 12. Cumulative damage for case f2w9.

Figure 13. Cumulative damage for case f4w6 with 1232 subgrade.

mate substantially different pavement lives for the same strain conditions.

A close review of the values in Table 13 illustrates a variety of interesting occurrences:

1. Cases with Mn/ROAD test section ML5-F-4 that employed the lower density subgrade (f4w6ld) or the "1232" subgrade (f4w6ss) predicted the pavement to fail much more quickly than when the higher (optimum) density 1206 subgrade was used. This is due to the fact that the higher density "1206" subgrade used in most simulations maintained a resilient modulus during the summer months in excess of 276,000 kPa (40,000 lb/in.^{2}), but the modulus values for the same period were about 96,000 kPa (14,000 lb/in.^{2}) for f4w6ld and about 6900 kPa (1000 lb/in.^{2}) for f4w6ss. The "low density" predicted moduli are the closest to the values measured during the summer months with an FWD.

2. Variations in water table position in the same test section result in different predicted lifespans, especially if the water table is less than 3 m (10 ft) deep at one location and more than 6 m (20 ft) deep at another. Both the ML5-F-2 and ML5-F-3 test section simulations illustrate a shorter predicted life with a shallow water table depth. For the shallow water table conditions, greater availability of water results in higher thaw weakening (reduced modulus values) in the spring.

3. Most of the sections are predicted to fail due to cracking of the pavement caused by tensile stresses at the bottom of the pavement much before they will fail due to rutting caused by excessive deformation of the subgrade. It is only the simulations of the full-depth sections (ML5-F-4, case f4w6, and ML10-F-14, f14w50) that indicate rutting failures may occur before excessive fatigue cracking.

Figures 11 to 13 illustrate examples of the relation between accumulating damage and time. Additional plots of heave, frost penetration, and cumulative damage for all the flexible sections are compiled in Appendix A.

Damage related to the horizontal strain criteria has different patterns with time for different models. Damage predicted by the MS-1 (Asphalt Institute) model has some increase during winter thaw events and during the main spring thaw, but a majority of its increase is in the summer period. Damage from the MS-11 (Asphalt Institute) model has a consistent pattern of rising during winter and spring thaw periods, and remaining constant during the summer. The pat-

Table 14. Applications to failure (× 1000) from simulations of rigid test sections.

Case	RCON = 650 SCI = 80	RCON = 500 SCI = 80	RCON = 650 SCI = 90
5-YEAR			
R5W6	52,601	507	45,244
R5W12	65,598	605	56,452
R6W4	157,655	1,505	135,622
R6W12	132,120	1,701	113,933
10-YEAR			
R11W6	$>5.6 \times 10^8$	18,761,000	$>5.6 \times 10^8$
R11W12	$>5.6 \times 10^8$	28,141,500	$>5.6 \times 10^8$

Notes:

RCON = Concrete flexural strength (lb/in.^{2})

SCI = Surface condition index at failure

Traffic simulated at rate of 562,830 ESAL applications/yr.

tern of damage accumulation from the Corps of Engineers model is similar to the MS-1 model, especially when the water table is shallow, causing larger resultant deflections and strains. For simulations with deeper water tables, smaller amounts of damage accumulate during the summer.

Damage from models using the vertical strain criteria follow three general patterns: 1) a sharp rise during spring thaw period with no accumulation at other times of the year (e.g., Fig. 12), 2) a series of increases during winter thaw events and the spring thaw (Fig. 11), and 3) in the cases with lower modulus subgrades, a gradual increase in damage during the spring, with sharper increases in the summer (Fig. 13). This last result is likely due to the anomalously low asphalt moduli being predicted by the Schmidt model.

Results—rigid sections

Predicted applications to failure for the concrete (rigid) sections is shown in Table 14, with the three sections in the table indicating the results of a sensitivity study. In the left-hand section, the flexural strength of the concrete was set at 4480 kPa (650 lb/in.^{2}) and the surface condition index (SCI) at the point of failure was set at 80. In the central section, the flexural strength was reduced to 3448 kPa (500 lb/in.^{2}), while the SCI remained at 80. For predictions in the right-hand column, the flexural strength was kept at

4480 kPa and the SCI was increased to 90. A comparison of the cumulative damage with time for the case representing section ML5-R-5 with a 1.8-m (6-ft) water table (r5w6) using all three combinations of flexural strength and SCI is also illustrated in Figure 14. Appendix B has a compilation of graphs depicting the frost/thaw penetration and cumulative damage for all rigid sections simulated.

Cases with a flexural strength of 4480 kPa exhibited very little damage, with the ML10-R-11 section having unmeasurable damage. Reducing the flexural strength to 3448 kPa greatly increased the predicted damage for the 5-year sections, but had a lesser effect on damage in the 10-year section.

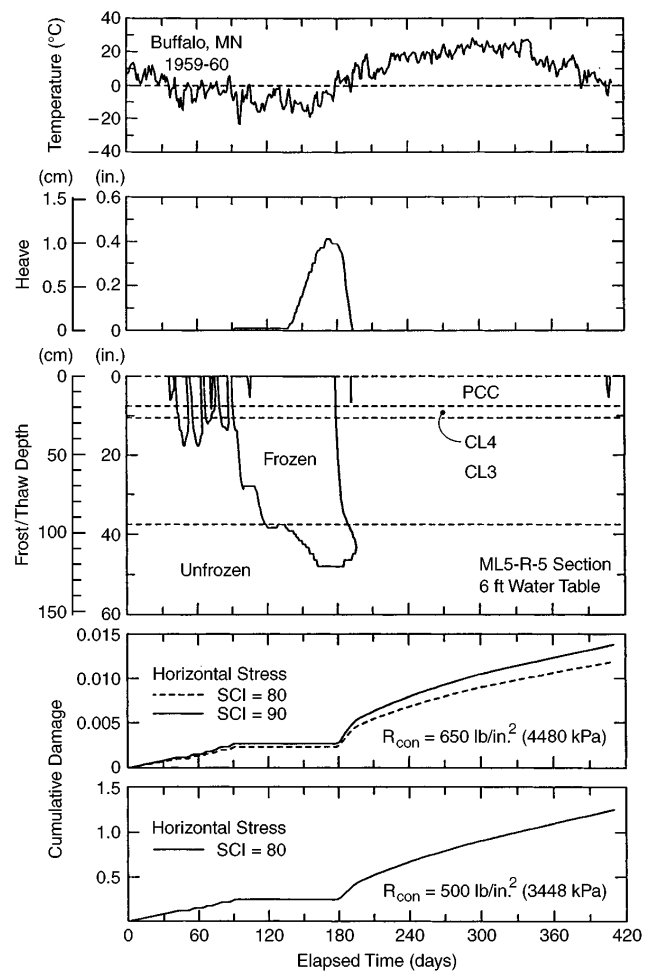The pattern of damage accumulation with time varied with the test section simulated

Figure 14. Cumulative damage for case r5w6.

24

(App. B). ML5-R-5 experienced rapid increases in damage during the thaw periods, but also had an equivalent increase in damage over the summer months. The other sections experienced a majority of their damage during the thaw periods and very little damage during the summer.

The low damage predictions result from the fact that the model predicts damage at the center of a slab, whereas the majority of damage occurs at the slab edges. Chou (1989) recommends increasing the stresses computed from the layered elastic method by a factor of 1.33 to estimate the coverage levels for roadway pavements.

Phase 2A

To address problems discovered in the Phase 1 modeling series, three additional simulation series were conducted on the eight flexible test sections studied in Phase 1 with the water table located at the shallowest position. A change that applied to all three series was that the normalized volumetric unfrozen water content form of the frozen modulus equations (Table 10a) was used, rather than the normalized gravimetric form used in Phase 1.

The first of the new series was essentially a repeat of the initial series in that it used the Schmidt model (eq 8) for calculation of the asphalt modulus and the high density 1206 form of the subgrade for modulus calculations. It differed from the initial series in that the normalized volumetric unfrozen water content form of the frozen modulus equations was utilized. A mistake in the CUMDAM program was also remedied—correcting the value of the subgrade modulus used in the Corps of Engineers vertical strain damage calculation. Table 15 lists the results of this series in the rows labeled "Schmidt." In general, predictions of applications to failure in the conventional cross sections were less than in the original series using the horizontal strain criteria and greater using the vertical strain criteria. In the full-depth sections (F4 and F14), applications to failure were increased in both the horizontal and vertical strain criteria.

The second series addressed the issue that the Phase 1 simulations computed summer asphalt moduli that were lower than considered reasonable. In this series, the Ullidtz model (eq 9) was used to calculate the asphalt modulus at temperatures greater than 1°C; at colder temperatures, the

Schmidt model was used. This series also used the high density 1206 form for the subgrade modulus calculations. Results for this series are shown in Table 15 in rows labeled "Ullidtz." In nearly all cases, this series produced higher predicted applications to failure than the corresponding Schmidt series.

The third series also used the Ullidtz model to calculate the asphalt modulus. In addition, it addressed the problem from the Phase 1 simulations that during the summer the predicted subgrade moduli based on the high-density 1206, or "normal" form were higher than FWD-measured values. For this series, the unfrozen subgrade modulus, when recovered, was set to be constant at 103,000 kPa (15,000 lb/in.[2]). This value was chosen as being approximately equal to an average value back-calculated from FWD measurements on subgrade during fall 1991.* As a result of this modulus approximation, the linear model (model 0 in Table 4) was used in NELAPAV for all subgrade calculations. The applications to failure from this series are listed in Table 15 as "Ull-15K." In the conventional sections including a base/subbase, the applications to failure were slightly lower than those resulting from the previous case with the Ullidtz asphalt model and the higher-modulus subgrade; in the full-depth sections, they were quite a bit lower.

A comparison of the Ullidtz/15K subgrade series results with the originally designed failure at 3,300,000 applications for the 5-year sections and at 6,600,000 applications for the 10-year sections yields the following conclusions:

1. In general, the Mechanistic Pavement Design Procedure predicts the 5-year conventional sections to fail due to asphalt cracking prior to the end of the design life, while failure from subgrade rutting is predicted beyond the design life.

2. Predictions for the 5-year full-depth section indicate that it will not fail from asphalt cracking, but two of the three criteria for subgrade rutting indicate early failure.

3. The two 10-year conventional sections with class 5 and class 6 special bases (F21 and F22) are predicted to fail from asphalt cracking at about the end of the design applications, while subgrade rutting criteria indicate longer life.

_____

* D. Van Deusen, Mn/ROAD, pers. comm. 1992.

Table 15. Predicted applications to failure ($\times$ 1000) from simulations of flexible test sections run in Phase 2A series.

Cases		Asp. Inst. MS-1	Asp. Inst. MS-11	Corps of Engineers	Coetzee/ Connor	Asp. Inst. MS-1	Corps of Engineers	FAA
		Horizontal criteria				*Vertical criteria*		
5-YEAR								
F1W9								
	Phase 1	86	498	88	4,380	136,942	5,653	11,879
	Schmidt	85	414	78	3,557	244,709	3,297	15,665
	Ullidtz	651	935	218	17,616	258,179	3,430	17,025
	Ull-15K	617	863	201	15,578	213,193	3,133	18,441
F2W9								
	Phase 1	522	1,244	550	42,703	32,477	1,345	1,526
	Schmidt	271	859	259	14,634	210,011	2,840	11,389
	Ullidtz	970	1,429	376	37,053	255,832	3,262	15,488
	Ull-15K	908	1,303	340	31,925	117,747	1,971	6,649
F3W8								
	Phase 1	957	1,706	958	92,419	116,287	2,653	9,611
	Schmidt	533	1,224	487	32,818	96,046	1,197	7,298
	Ullidtz	1,255	1,842	528	58,812	87,260	1,108	6,381
	Ull-15K	1,225	1,705	503	54,327	115,098	1,404	10,501
F4W6								
	Phase 1	28,585	75,751	90,926	$>10^7$	3,715	15	152
	Schmidt	45,171	121,039	175,884	$>10^7$	4,505	314	164
	Ullidtz	65,218	123,699	149,292	$>10^7$	11,952	317	246
	Ull-15K	7,055	26,561	8,219	3,752,200	7,996	331	467
10-YEAR								
F14W50								
	Phase 1	103,272	485,198	605,194	$>10^7$	8,602	10	251
	Schmidt	126,479	721,577	970,397	$>10^7$	11,687	417	336
	Ullidtz	209,230	760,581	852,773	$>10^7$	17,107	412	359
	Ull-15K	19,902	153,779	40,903	$>10^7$	26,943	787	2,232
F19W18								
	Phase 1	396	6,148	966	75,751	2,962,263	56,680	457,585
	Schmidt	309	4,335	635	43,328	4,329,462	37,175	632,393
	Ullidtz	2,948	14,480	2,278	574,316	4,329,462	37,422	639,580
	Ull-15K	2,688	12,367	1,976	469,025	1,125,660	18,173	264,239
F21W18								
	Phase 1	3,394	30,456	12,751	2,010,107	562,830	84,382	42,478
	Schmidt	1,958	16,072	4,701	420,022	865,892	10,452	70,442
	Ullidtz	8,515	33,402	9,343	3,752,200	792,718	9,689	61,849
	Ull-15K	6,661	23,335	6,513	2,345,125	457,585	8,752	66,686
F22W45								
	Phase 1	7,614	57,315	31,147	8,040,429	73,190	22,415	3,388
	Schmidt	1,750	21,507	5,070	493,711	68,388	1,078	3,077
	Ullidtz	8,235	42,964	9,192	3,752,200	85,667	1,278	4,297
	Ull-15K	6,186	26,045	5,986	2,084,556	120,520	2,086	9,840

Notes:

Phase 1—previous work, Schmidt— new series with Schmidt asphalt model, Ullidtz—new series with Ullidtz asphalt model above 1°C, Ull-15K—new series with Ullidtz asphalt model and summer subgrade modulus = 15K lb/in.^{2} (103,000 kPa). Traffic simulated at rate of 562,830 ESAL applications/yr.

4. The 10-year conventional section with class 3 special subbase (F19) may fail due to asphalt cracking, but not from subgrade rutting.

5. Predictions for the 10-year full-depth section indicate that it will not fail from asphalt cracking, but two of the three criteria for subgrade rutting indicate early failure.

Phase 2B

To investigate the influence of the applied freeze/thaw season on the predicted performance of the sections, an environmental effects sensitivity series was conducted using the single conventional flexible test section, F3, which included class 5 special and class 3 special materials as its base and subbase courses (Fig. 6) and a water table at a depth of 2.4 m (8 ft). Prior simulations had applied upper boundary temperatures from the season with a freezing index near to the 30-year mean, 1959–60 (freezing index 1003 °C-days, 1806 °F-days). This new series applied temperatures from three other freeze/thaw seasons, including those with freezing indices equal to the mean of the three coldest seasons during the period 1959 to 1987 and the maximum and minimum for the 1959–1987 period. These seasons were maximum—1978–79 (1477 °C-days, 2658 °F-days), minimum—1986–87 (467 °C-days, 841

°F-days), and mean 3 coldest out of 30—1964-65 (1391 °C-days, 2503 °F-days). Results from these years were compared with F3W8 predictions for the mean year that had been run in the "Schmidt" series, since this Phase 2B series also used the Schmidt model for asphalt modulus calculations (eq 8) and the high density 1206 form for the subgrade modulus calculations.

Figure 15 shows the freeze/thaw penetration in the F3 section predicted by FROST for all four freeze seasons. In the mean year, multiple small freeze/thaw events were followed by a long freeze event that penetrated the subgrade and a spring warming that remained above freezing. The minimum year had several freeze/thaw events, but they were less severe—none of them penetrated beyond the base course materials. The maximum year began with a very severe freeze event that penetrated to the subgrade and lasted all winter. In the spring, thawing of this freeze bulb was interrupted by two smaller freeze events, such that there existed a thawed layer in the subbase between two frozen zones. The year with a freezing index equal to the mean of the three coldest in 30 (3/30 year) had a freeze season consisting of a single severe freeze event that penetrated into the subgrade, which then thawed with no small freeze events.
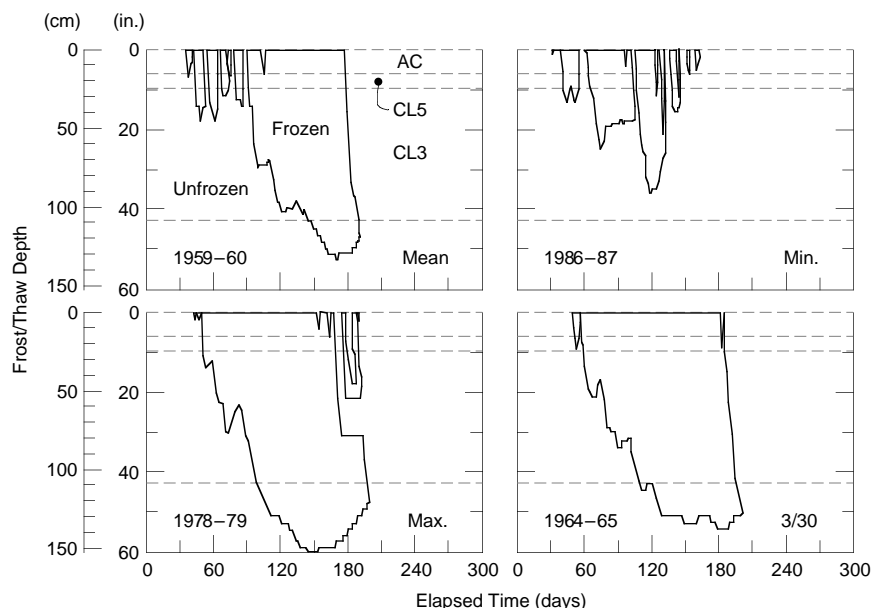

Figure 15. Frost and thaw penetrations predicted by FROST for freeze seasons in Phase 2B environmental sensitivity study. Simulations start on 1 October.

27

Table 16. Performance predictions for F3 test section with water table at 2.4 m (8 ft). Freeze/ thaw seasons applied as upper boundary temperatures were mean year—1959–60, maximum year—1978–79, minimum year—1986–87, average of the 3 coldest out of 30—1964–65.

	Applications to failure ($\times$ 1000)			
Failure criteria	Mean	Max	Min	3/30
Horizontal				
Asphalt Institute (MS-1)	533	384	573	397
Asphalt Institute (MS-11)	1,224	1,215	1,117	1,445
Corps of Engineers	487	375	593	368
Coetzee/Conner	32,818	25,284	50,660	23,530
Vertical				
Asphalt Institute (MS-1)	96,046	51,120	$>10^7$	96,046
Corps of Engineers	1,197	600	$>10^7$	1,143
FAA	7,298	4,080	$>10^7$	7,625

Note: Traffic simulated at rate of 562,830 ESAL applications/yr.

Table 16 lists the predicted damage in terms of applications to failure from this environmental series, in which traffic was simulated at 562,830 ESALs per year. Compared with the mean year, failure due to the horizontal strain criteria (asphalt cracking) is predicted earlier with the maximum year and the 3/30 year, and later with the minimum year. However, the spread of values is not that great, and 3 of the 4 models predict failure sooner than the design figure of 3,300,000 applications for all four of the seasons modeled. Time of failure due to the vertical strain criteria (asphalt rutting) is predicted sooner in the maximum year than the mean year, and at about the same time as the mean year with the 3/30 year. No damage due to subgrade rutting was predicted with the minimum year in which no frost penetrated the subgrade.

Phase 3

The third phase of the study modeled two flexible pavement sections to which 21 years of environmental conditions were applied. Various analyses were conducted attempting to correlate the predicted damage with the characteristics of the freeze seasons simulated.

Cross sections/material properties

The two cross sections simulated employed layer thicknesses from two Mn/ROAD test sections (Table 7). The first, section F4, was a "full-depth" section consisting of an asphalt layer lying directly above the lean clay subgrade. The second, section F3, was a "conventional" section, including class 6 special as the base material (substituted for class 5 special in the actual pavement structure) and class 3 special as the subbase.

Physical properties used for the materials were the same as shown in Table 13, with the exception that a lower density (1.69 Mg/m^3; 105.5 lb/ft^3) was used for the 1206 subgrade. Figure 16 illustrates predicted moduli for several densities of the 1206 subgrade. The asphalt modulus was calcu-
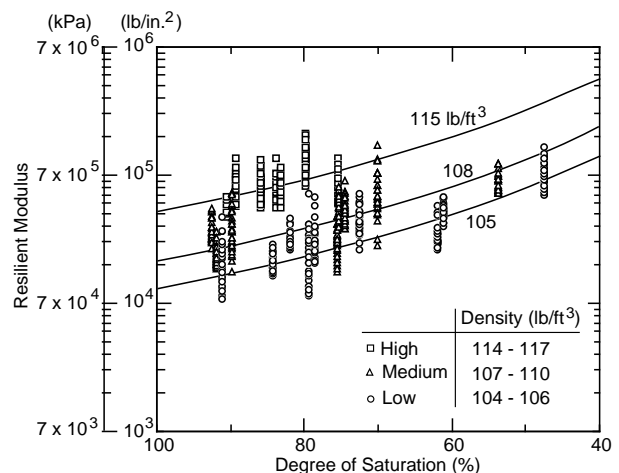

Figure 16. Resilient modulus vs. degree of saturation of never-frozen 1206 subgrade material illustrating the effect of dry density.

28

lated with a combination of the Ullidtz model at above 1°C temperatures and the Schmidt model at colder temperatures.

Environmental conditions

The series simulated the 21-year time period 1969–70 to 1989–90, using a combination of recorded air temperatures and an estimated position of the water table. The simulations started on 1 October of the first year and proceeded for 365 days, using mean daily air temperatures recorded at Buffalo, Minnesota, applied as a step condition for 24-hr periods. The depth to the water table was varied based on the total precipitation accumulated at St. Cloud, Minnesota, during the thaw season prior to the simulated freeze season. An inverse relationship between precipitation and

water table depth was applied such that the maximum precipitation produced the shallowest water table at 0.91 m (3 ft) below the surface and the minimum precipitation produced the deepest water table at 1.82 m (6 ft). The water table was held constant throughout the simulation at the depth determined by this relationship. Figure 17 shows the distribution of estimated water table and freeze index for this period.

Results

As in previous simulation series, there was a wide variation in the damage amounts predicted by the different models (Table 17). In general, less damage related to horizontal strain was predicted in the full-depth design than in the conventional design. On the other hand, when all other

Table 17. Results of 21-year freezing index/water table series.

| | | | | Maximum | Applications to failure (millions) | | | |
| | Water table depth | Freezing index | Freeze/thaw events in | freeze depth into subgrade | Horizontal strain Asphalt cracking | | Vertical strain Subgrade rutting | |
Year	m (ft)	°C (°F)-days	subgrade	(cm)	CEH	AIH-MS11	CEV	AIV-MS1
A. Full depth (F4)								
6970	1.5 (4.8)	1191 (2144)	2	91.8	18.20	66.00	0.21	5.38
7071	1.3 (4.2)	1152 (2074)	4	91.8	18.02	52.59	0.34	8.23
7172	1.1 (3.6)	1274 (2294)	2	91.8	15.16	45.02	0.31	7.64
7273	1.2 (4.0)	839 (1510)	2	69.8	18.97	50.69	0.37	7.72
7374	1.3 (4.2)	923 (1661)	2	77.8	17.80	51.48	0.78	10.97
7475	1.4 (4.6)	968 (1743)	3	81.8	17.21	47.93	0.18	5.47
7576	1.3 (4.2)	931 (1675)	3	73.8	16.83	52.26	0.16	4.15
7677	1.6 (5.3)	1256 (2261)	4	107.8	17.92	62.38	0.16	4.87
7778	1.1 (3.7)	1331 (2395)	1	91.8	13.88	60.22	0.10	3.01
7879	1.2 (3.8)	1477 (2658)	3	99.8	17.66	51.36	6.66	17.18
7980	1.2 (3.8)	903 (1625)	5	79.8	16.67	43.10	0.19	5.30
8081	1.2 (4.0)	666 (1199)	3	67.8	17.15	42.63	0.26	7.72
8182	1.8 (6.0)	1227 (2209)	3	107.8	16.29	47.92	0.04	1.44
8283	1.2 (3.9)	589 (1061)	8	63.8	16.73	34.26	0.11	3.71
8384	1.0 (3.3)	1179 (2123)	2	81.8	16.86	48.96	0.12	3.50
8485	1.0 (3.3)	942 (1696)	3	81.8	16.08	44.68	0.15	4.31
8586	1.0 (3.2)	1197 (2154)	2	81.8	17.67	71.27	0.79	11.48
8687	0.9 (3.0)	467 (841)	4	45.8	15.91	33.52	0.48	8.44
8788	1.5 (4.8)	898 (1616)	4	87.8	16.91	48.28	0.34	6.15
8889	1.5 (4.9)	1032 (1858)	4	87.8	17.57	50.53	0.26	7.19
8990	1.4 (4.7)	750 (1350)	7	65.8	16.50	37.45	0.25	6.83

Notes:
  CEH = Corps of Engineers (horizontal)   CEV = Corps of Engineers (vertical)
  AIH-MS11 = Asphalt Institute (MS-11)   AIV = Asphalt Institute (MS-1)
  ND = no damage
 Traffic simulated at rate of 660,000 ESAL applications/yr.

Table 17 (cont'd). Results of 21-year freezing index/water table series.

Year	Water table depth m (ft)	Freezing index °C (°F) days	Freeze/thaw events in subgrade	Maximum freeze depth into subgrade (cm)	Applications to failure (millions)			
					Horizontal strain Asphalt cracking		Vertical strain Subgrade rutting	
					CEH	AIH-MS11	CEV	AIV-MS1
A B. Conventional (F3)								
6970	1.5 (4.8)	1191 (2144)	1	13.4	0.46	2.46	0.82	61.97
7071	1.3 (4.2)	1152 (2074)	1	13.4	0.56	2.63	0.47	34.83
7172	1.1 (3.6)	1274 (2294)	1	17.4	0.56	2.53	0.34	26.17
7273	1.2 (4.0)	839 (1510)	0	0	0.49	1.69	ND	ND
7374	1.3 (4.2)	923 (1661)	2	1.4	0.46	2.04	ND	ND
7475	1.4 (4.6)	968 (1743)	1	5.4	0.49	2.61	1.46	120.66
7576	1.3 (4.2)	931 (1675)	1	0	0.55	2.71	ND	ND
7677	1.6 (5.3)	1256 (2261)	1	25.4	0.43	2.18	0.71	58.36
7778	1.1 (3.7)	1331 (2395)	1	13.4	0.49	2.31	0.51	38.69
7879	1.2 (3.8)	1477 (2658)	1	21.4	0.49	2.72	0.36	27.68
7980	1.2 (3.8)	903 (1625)	1	5.4	0.52	1.87	0.44	33.62
8081	1.2 (4.0)	666 (1199)	0	0	0.50	1.50	ND	ND
8182	1.8 (6.0)	1227 (2209)	1	29.4	0.42	2.21	0.46	37.95
8283	1.2 (3.9)	589 (1061)	0	0	0.51	1.34	ND	ND
8384	1.0 (3.3)	1179 (2123)	1	5.4	0.49	1.84	1.18	91.16
8485	1.0 (3.3)	942 (1696)	1	5.4	0.48	1.56	0.98	77.74
8586	1.0 (3.2)	1197 (2154)	1	5.4	0.48	2.70	1.64	ND
8687	0.9 (3.0)	467 (841)	0	0	0.44	1.45	ND	ND
8788	1.5 (4.8)	898 (1616)	1	9.4	0.45	1.85	0.72	58.30
8889	1.5 (4.9)	1032 (1858)	1	9.4	0.53	1.89	0.45	33.69
8990	1.4 (4.7)	750 (1350)	0	0	0.55	1.65	ND	ND

Notes: CEH = Corps of Engineers (horizontal)   CEV = Corps of Engineers (vertical)
AIH-MS11 = Asphalt Institute (MS-11)   AIV = Asphalt Institute (MS-1)
ND = no damage
Traffic simulated at rate of 660,000 ESAL applications/yr.
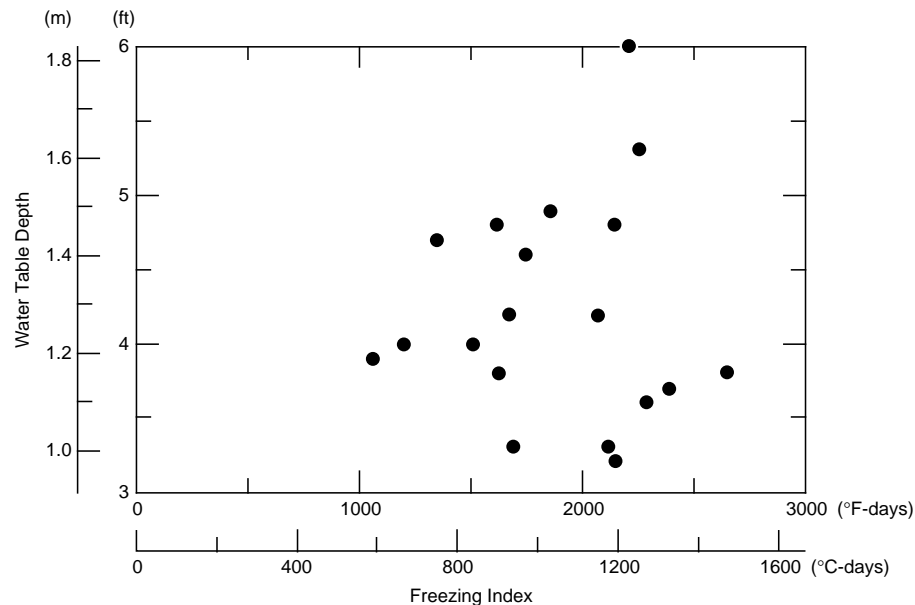
Figure 17. Distribution of freezing indices and water table depths in 21-year Phase 3 series.

30

conditions are constant, there was more damage related to vertical strain in the full-depth design. When frost did not penetrate the subgrade in the conventional design, essentially no vertical strain damage was predicted.

Freeze season characteristics were initially quantified by analyzing the total freezing index, the number of times that frost was predicted to enter the subgrade and the maximum depth of frost penetration beneath the top of the subgrade (Table 17). Lower amounts of damage (higher applications to failure) were predicted by the Asphalt Institute horizontal strain model in seasons with higher freezing indices and deeper frost penetration in both the full-depth and conventional cross sections. However, predictions of damage from the other models did not correlate with any of the above parameters.

It was noted that two similarly categorized seasons, 1983–84 and 1985–86, which had nearly identical freezing indexes and water table depths, as well as the same number of freeze thaw events, had diversely different damage predictions in the full-depth section (Table 17a). A large thaw event in the middle of the 1983–1984 freeze season was accompanied by severe weakening of the subgrade both during midwinter and spring thaw, which resulted in a considerable amount of predicted damage (Fig. 18). The 1985–86 year experienced a nearly continuous freeze season with no significant midwinter thaw event (Fig. 19). As a result, the subgrade modulus underwent thaw weakening
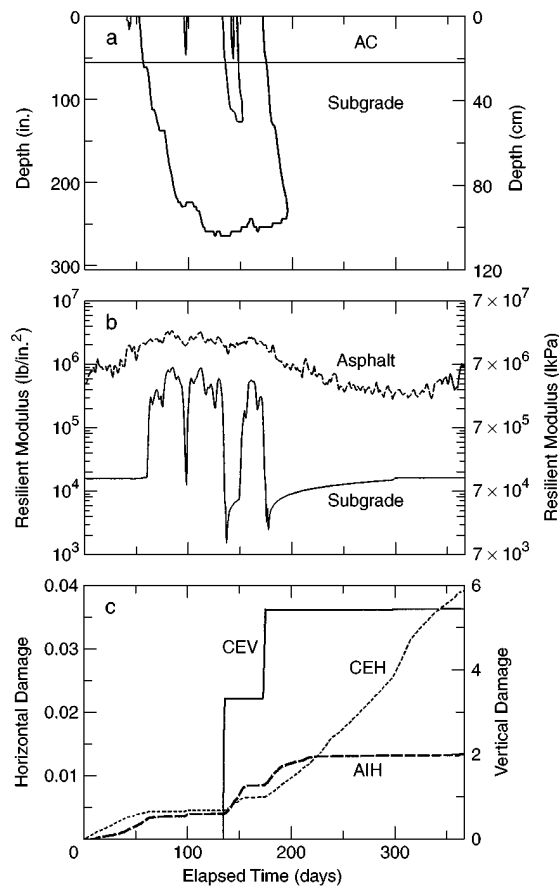

Figure 18. Predicted results from simulation of full-depth section during freeze season 1983–1984, starting on 1 October. a) Frost/thaw depth, b) seed resilient modulus passed to NELAPAV, and c) cumulative damage. (Abbreviations—see Table 17.).
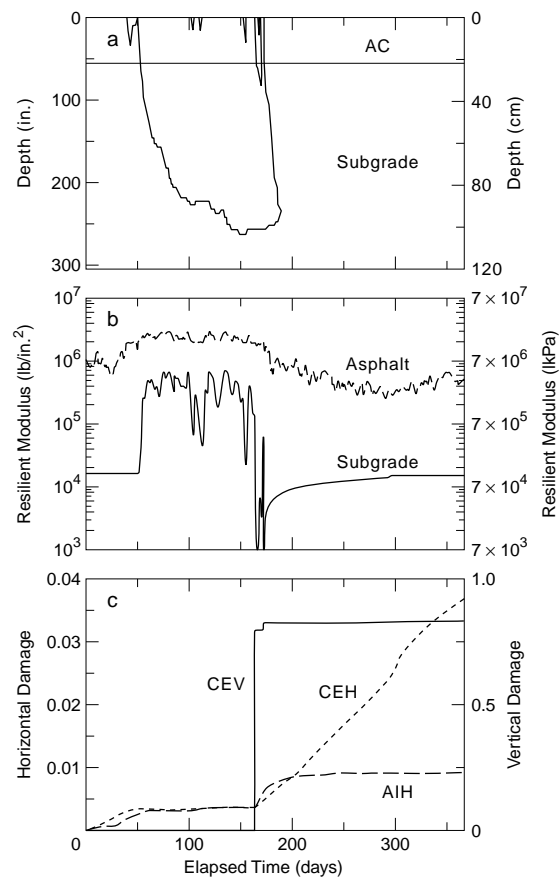

Figure 19. Predicted results from simulation of full-depth section during freeze season 1985–1986, starting on 1 October. a) Frost/thaw depth, b) seed resilient modulus passed to NELAPAV, and c) cumulative damage (see Table 17).

only during spring thaw in the 1985–86 season, and the corresponding total damage accumulation was much less.

Based on the above observation, we tried a new approach to quantifying the characteristics of the freeze seasons. It involved summing the thawing degree days experienced during the freeze season in two ways. The first was a total from all events, and the second was a total from only the thaw events that exceeded 16°C-days (30°F-days) (Table 18). The quantity 16°C-days was chosen based on analysis by Mahoney et al. (1985) indicating that pavements approach their critically weak condition after this amount of thaw has been experienced. Unfortunately, neither of these quantities correlated with predicted damage amounts. Ap-

parently, a more sophisticated index that perhaps combines freeze index, severity of midwinter thaw events, and other parameters is required to correlate with predicted damage.

In analyzing the Phase 3 simulation results, we examined the distribution of predicted damage through the four seasons defined as follows: fall—1 October to start of freeze, winter—freeze season as defined by freezing index, spring—75 days following end of freeze season, summer—remainder of 365-day simulation. The simulations predicted a wide variation in seasonal damage amounts for different years, especially in the vertical strain damage in the conventional cross section (Fig. 20). In years when vertical strain damage was predicted for the conventional cross
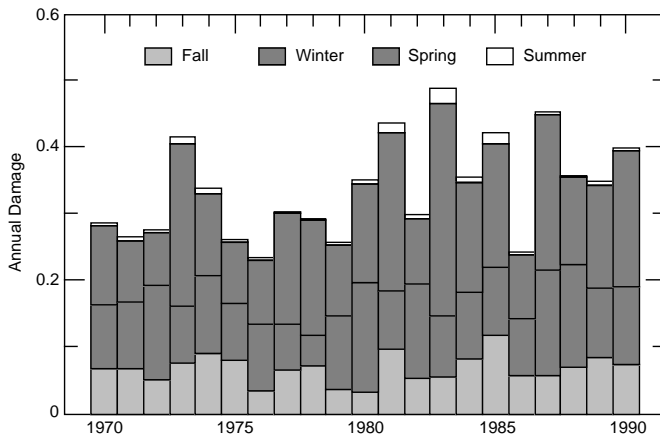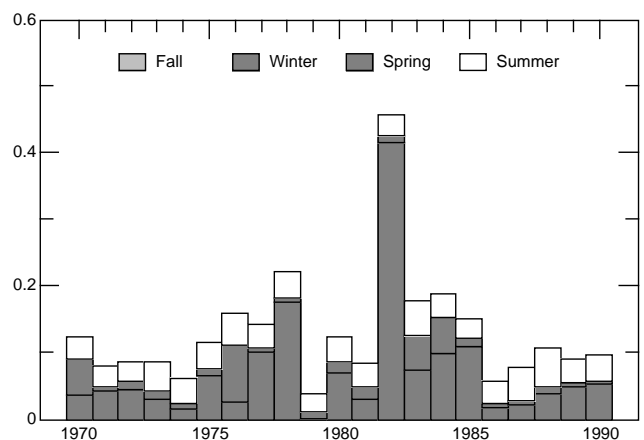

a. Conventional section, Asphalt Institute horizontal strain model MS-11.
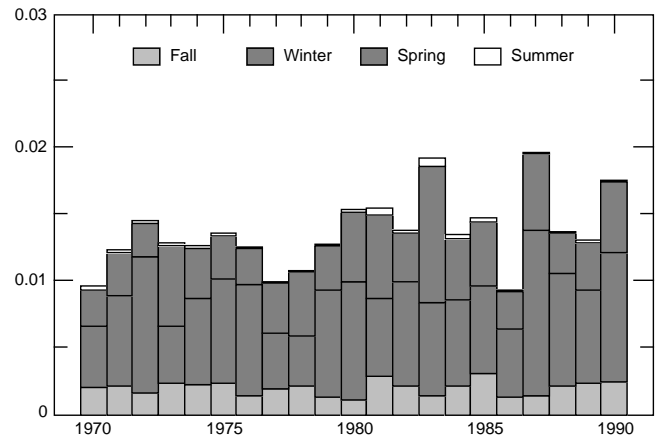
c. Full depth section, Asphalt Institute horizontal strain model MS-11.
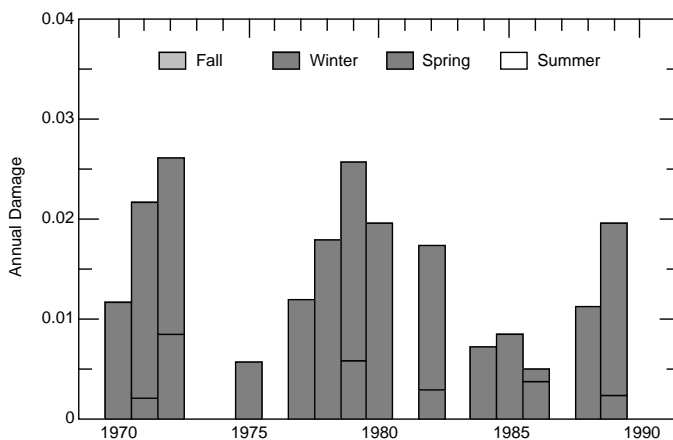
b. Conventional section, Asphalt Institute vertical strain model MS-1.

d. Full depth section, Asphalt Institute vertical strain model MS-1.

Figure 20. Distribution of cumulative damage during seasons.

Table 18. Midwinter thaw index summations.

Year	Water table depth m (ft)	Freezing index °C(°F)-days	Midwinter thaw index (Total) °C(°F)-days	(> 30 DD) °C(°F)-days
6970	1.5 (4.8)	1191 (2144)	25.5 (45.9)	0.0
7071	1.3 (4.2)	1152 (2074)	41.0 (73.8)	0.0
7172	1.1 (3.6)	1274 (2294)	50.0 (90.0)	19.4 (35.0)
7273	1.2 (4.0)	839 (1510)	21.5 (38.7)	0.0
7374	11.3 (4.2)	923 (1661)	56.0 (100.8)	22.3 (40.1)
7475	1.4 (4.6)	968 (1743)	35.0 (63.0)	14.2 (25.5)
7576	11.3 (4.2)	931 (1675)	67.0 (120.6)	20.7 (37.2)
7677	1.6 (5.3)	1256 (2261)	44.0 (79.2)	0.0
7778	1.1 (3.7)	1331 (2395)	26.5 (47.7)	0.0
7879	1.2 (3.8)	1477 (2658)	52.0 (93.6)	18.0 (32.4)
7980	1.2 (3.8)	903 (1625)	32.0 (57.6)	0.0
8081	1.2 (4.0)	666 (1199)	41.0 (73.8)	17.5 (31.5)
8182	1.8 (6.0)	1227 (2209)	31.5 (56.7)	21.9 (39.4)
8283	11.2 (3.9)	589 (1061)	92.5 (166.5)	75.0 (135.0)
8384	1.0 (3.3)	1179 (2123)	40.0 (72.0)	34.7 (62.4)
8485	1.0 (3.3)	942 (1696)	40.0 (72.0)	22.9 (41.2)
8586	1.0 (3.2)	1197 (2154)	29.0 (52.2)	0.0
8687	10.9 (3.0)	467 (841)	65.0 (117.0)	40.1 (72.1)
8788	11.5 (4.8)	898 (1616)	79.0 (142.2)	54.2 (97.6)
8889	1.5 (4.9)	1032 (1858)	49.0 (88.2)	0.0
8990	11.4 (4.7)	750 (1350)	70.5 (126.9)	27.0 (48.6)

Table 19. Average percentage of total yearly damage accumulated during four seasons.

Section/model	Accumulated damage (% of total) Fall	Winter	Spring	Summer
Conventional				
AIH	22	31	45	2
AIV	0	40	60	0
CEV	0	42	58	0
Full depth				
AIH	16	51	32	1
AIV	2	44	16	38
CEV	0	80	20	0

Notes:
  AIH = Asphalt Institute horizontal (MS-11)
  AIV = Asphalt Institute vertical (MS-1)
  CEV = Corps of Engineers vertical

section, a majority occurred in the spring, while the remainder occurred in the winter (Table 19). Horizontal strain damage in the conventional cross section also occurred mainly in the spring, with additional significant amounts in both the winter and fall, and very small amounts in the summer.

In the full-depth cross section, horizontal strain damage occurred primarily in the winter, with slightly less in the spring, and some additional damage in the fall. Both vertical strain models predicted damage in the full-depth section to occur mainly in the winter, with some in the spring. The Asphalt Institute vertical strain model also predicted additional amounts of summer damage.

DISCUSSION AND RECOMMENDATIONS

The Phase 1 modeling series indicated significantly different performance by the different test sections and highly variable results depending on the performance model applied (Table 13). The simulated performance of the test sections was also significantly affected by the subgrade conditions, e.g., density, soil moisture and water table depth. For example, compare the model predictions using the Asphalt Institute MS-1 horizontal strain criteria. For case f4w6, the full-depth 5-year section with the 1206 subgrade in its opti-

33

mum density condition, the model predicts 28,585,000 applications to failure. In case f4w6ld, the same test section with a low density value for the 1206 subgrade, the model predicts 1,905,000 applications to failure. And finally, in case f4w6ss, with the 1232 subgrade that produced lower resilient modulus values in lab tests, failure is predicted after only 72,000 applications, or in less than one year.

After the Phase 1 simulations were complete, the resilient modulus data from the 1206 subgrade were reviewed. A calibration error of unknown magnitude was discovered in the resilient modulus equipment used to measure the unfrozen modulus on that material. Modulus testing of the 1206 subgrade in the frozen condition and all testing on the other materials were conducted on a different machine, which passed its calibration checks. Comparing frozen and unfrozen resilient modulus test results from the 1206 subgrade with those from other materials tested, Figure 7, indicates that the unfrozen M_r values for the 1206 subgrade may be about an order of magnitude too high. A lower M_r for the 1206 subgrade would have resulted in earlier failures than computed in this report where the 1206 optimum density subgrade was used.

We are currently investigating the unfrozen 1206 subgrade results and will include findings and revised performance predictions in Berg (in prep.)

It is obviously extremely important to use the representative subgrade conditions in the design simulations. Results are consistent with observations from in-service pavements; e.g., weak areas fail much more rapidly than strong ones and high water tables cause failures before similar pavements constructed over lower water tables. Both the 1206 and 1232 subgrade samples were obtained from the test site and were located less than one-half mile apart, yet their tested behavior was quite different.

Another important aspect governing the results of the Mechanistic Pavement Design Procedure is the method used to calculate the asphalt concrete resilient modulus. The use of the Schmidt model, which produces extremely low summer season moduli, partially accounts for the short lifespans predicted in the Phase 1 modeling series. Replacement with the Ullidtz model in part of the Phase 2A modeling series increased the predicted lifespans of the sections when judged by the horizontal strain criteria (Table 15).

Results from the Phase 2A series that used the Ullidtz model for asphalt modulus calculations and a recovered summer subgrade modulus of 103,00 kPa (15,000 lb/in.^{2}), a close approximation of the value backcalculated from FWD measurements on subgrade during fall 1991, yield performance predictions that are as "fine-tuned" as possible, so far (Table 15 "Ull-15K"). When these Mechanistic Pavement Design Procedure predictions are compared with the originally designed failure at 3,300,000 applications for the 5-year sections and 6,600,000 applications for the 10-year sections, the following statements can be made:

1. Predictions for the full-depth sections, both 5 and 10 year, indicate that they will not fail from asphalt cracking, but two of the three criteria for subgrade rutting indicate early failure;

2. Conventional sections are predicted not to fail due to subgrade rutting; however, sections with more frost-susceptible bases are predicted to fail because of asphalt cracking relatively early in their design life, and sections with non-frost-susceptible bases are predicted to fail towards the end of their design life.

By modeling 21 years of environmental conditions in the Phase 3 series, we were hoping to find the characteristics of a "most severe" winter that could be used for design purposes. The results were complex and a relation between predicted failure and characteristics of freeze seasons was elusive, at best.

Based on the above results, we recommend the following studies:

1. The class 4 special and class 5 special base materials should receive the full complement of laboratory tests so that simulations may be run using properties of actual materials from the site rather those of substitute materials.

2. Once performance data are received from Mn/ROAD, predicted and measured values of moisture, temperature, and strains should be compared.

3. Use performance data from Mn/ROAD to revise, refine or develop new damage models for rutting and fatigue cracking.

4. Use performance data from Mn/ROAD to refine or develop a new model for the change of the asphalt modulus with temperature.

5. Use data from falling weight deflectometer tests on Mn/ROAD to estimate pavement performance on an annual basis.

6. The Procedure should be used to estimate performance of all of the test sections. This study evaluated less than one-half of the sections.

CONCLUSIONS*

The range of values produced for the various scenarios is, as noted, extremely wide. This leads to the conclusion that mechanistic design in its present stage, while a powerful predictor of changes in pavement response with changes in loads or moduli, is at present an uncertain predictor of pavement performance. Data and analyses from Mn/ROAD are crucial to improving that current uncertain state of performance prediction.
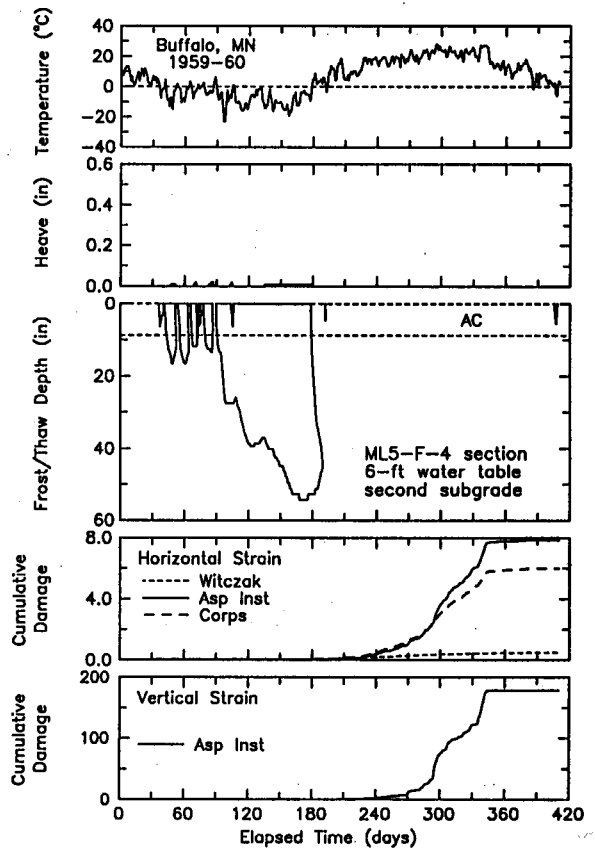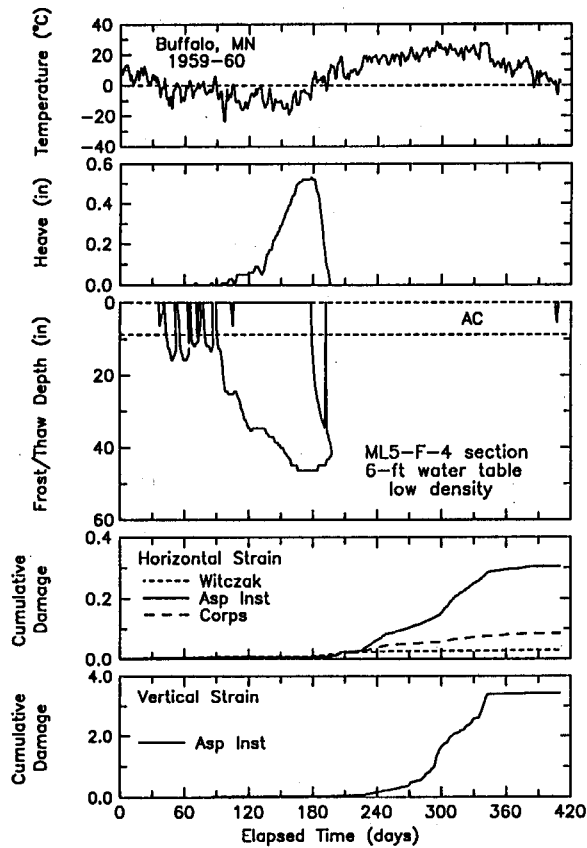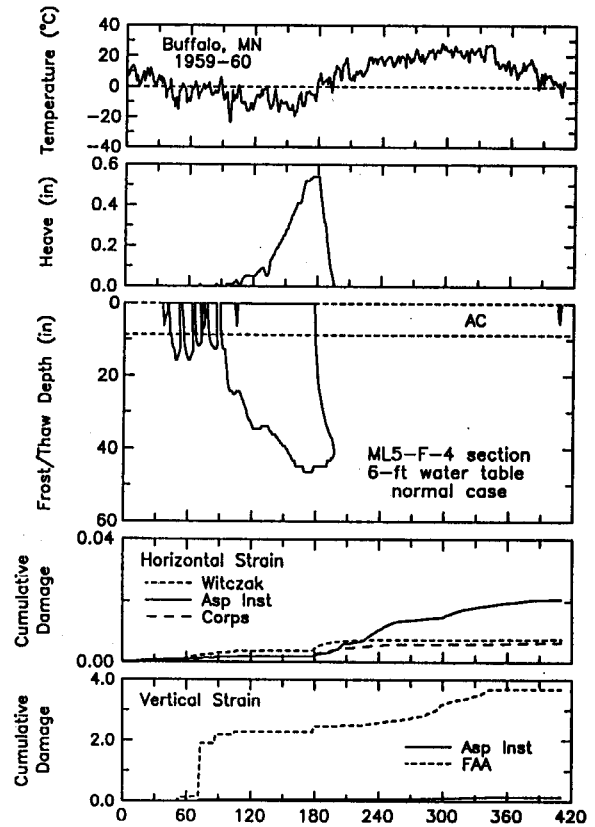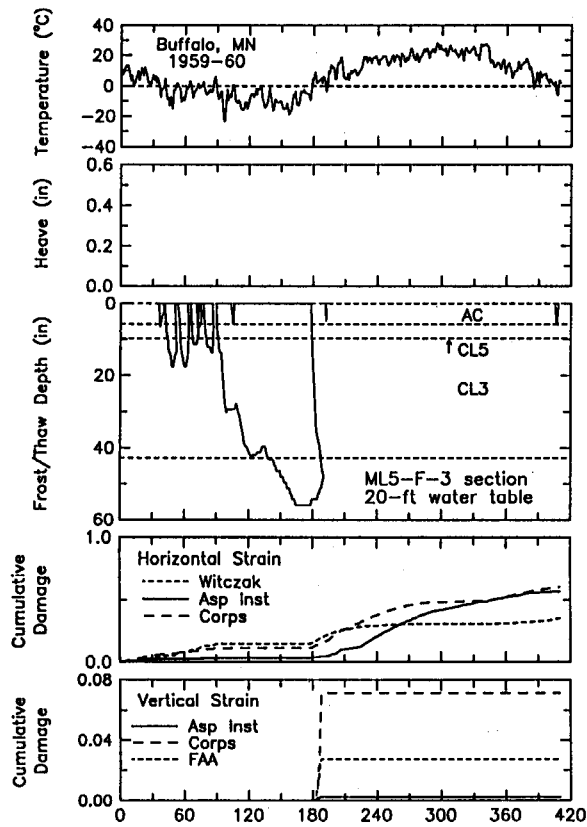
LITERATURE CITED

The Asphalt Institute (1982) Research and development of the Asphalt Institute's thickness design manual (MS-1), ninth edition. College Park, Maryland. Research Report No. 82-2.

R. Berg (in prep.) Resilient modulus testing of materials from Mn/ROAD, phase 2. USA Cold Regions Research and Engineering Laboratory, Special Report.

Berg, R.L., S.R. Bigl, J. Stark and G. Durrell (1996) Resilient modulus testing of materials from Mn/ROAD, Phase 1. USA Cold Regions Research and Engineering Laboratory, Special Report 96-19, Mn/DOT Report 96-21.

Berg, R.L., G.L. Guymon and T.C. Johnson (1980) Mathematical model to correlate frost heave of pavements with laboratory predictions. USA Cold Regions Research and Engineering Laboratory, CRREL Report 80-10.

Bigl S.R. and Berg, R.L. (1996a) Testing of materials from the Minnesota Cold Regions Pavement Research Test Facility. USA Cold Regions Research and Engineering Laboratory, Special Report 96-20, Mn/DOT Report 96-24.

Bigl S.R. and Berg, R.L. (1996b) Material test-
ing of initial pavement design modeling: Minnesota Road Research Project. USA Cold Regions Research and Engineering Laboratory, CRREL Report 96-14, Mn/DOT Report 96-23.

Bush, A. (1980) Non-destructive testing for light aircraft pavements. USAE Waterways Experiment Station, Vicksburg, Mississippi, sponsored by the Federal Aviation Administration.

Chamberlain, E., T.C. Johnson, R.L. Berg and D.M. Cole (in prep.) Prediction of pavement behavior under loading during freezing and thawing. USA Cold Regions Research and Engineering Laboratory, CRREL Report.

Chou, Y.T (1989) Development of failure criteria of rigid pavement thickness requirements for military roads and streets, elastic layered method. USAE Waterways Experiment Station, Vicksburg, Mississippi, Miscellaneous Paper GL-89-9.

Cole, D., D. Bently, G. Durell and T. Johnson (1986) Resilient modulus of freeze-thaw affected granular soils for pavement design and evaluation, Part 1. Laboratory tests on soils from Winchendon, Massachusetts, test sections. USA Cold Regions Research and Engineering Laboratory, CRREL Report 86-4.

Cole, D., D. Bently, G. Durell and T. Johnson (1987) Resilient modulus of freeze-thaw affected granular soils for pavement design and evaluation, Part 3. Laboratory tests on soils from Albany county airport. USA Cold Regions Research and Engineering Laboratory, CRREL Report 87-2.

Coetzee, N.F. and B.G. Connor (1990) Fatigue characteristics of Alaskan pavement mixes. Transportation Research Record No. 1269, Transportation Research Board, National Research Council, Washington D.C., p.168–175.

Gardner, W.R. (1958) Some steady-state solutions of the unsaturated flow equation with application to evaporation from a water table. *Soil Science*, **88**: 228–232.

Guymon, G.L., R.L. Berg and T.V. Hromadka (1993) Mathematical model of frost heave and thaw settlement in pavements. USA Cold Regions Research and Engineering Laboratory, CRREL Report 93-2.

Ingersoll, J. (1981) Method for coincidentally determining soil hydraulic conductivity and moisture retention characteristics. USA Cold Regions Research and Engineering Laboratory, Special Report 81-2.
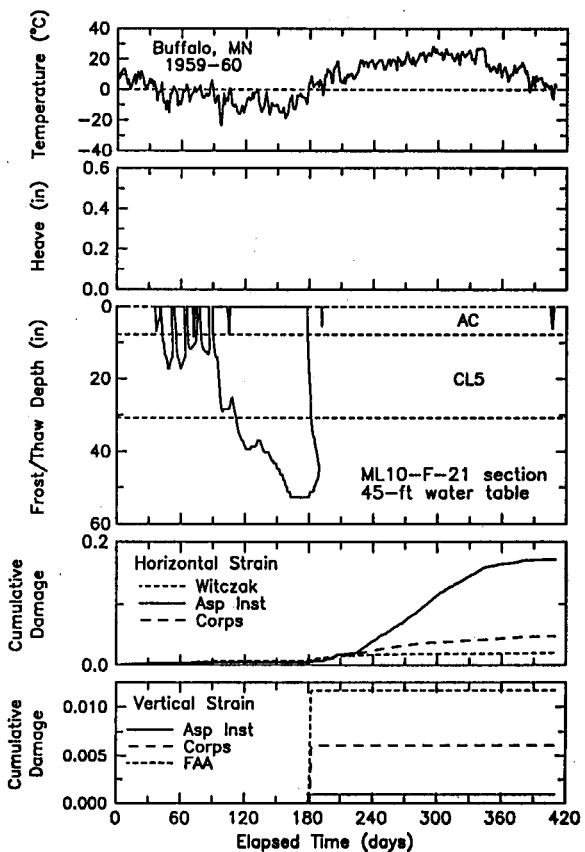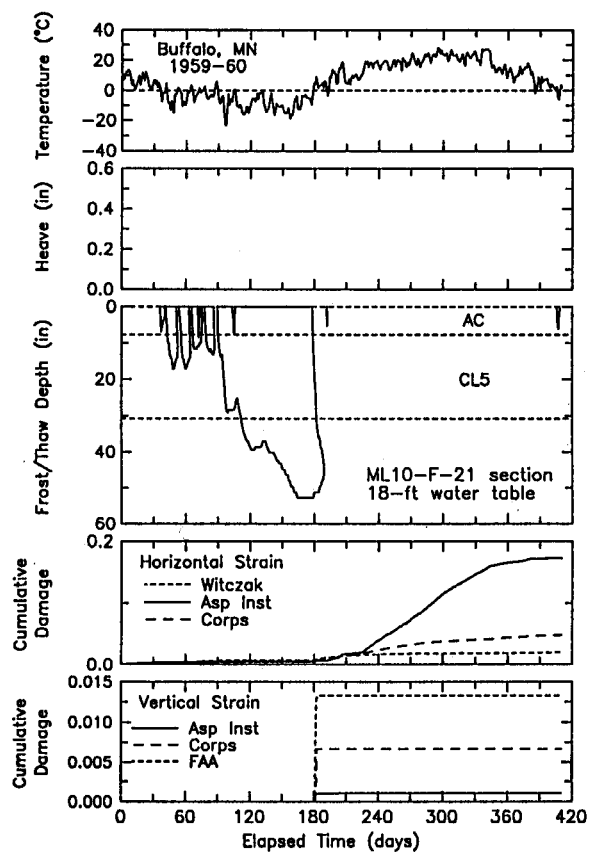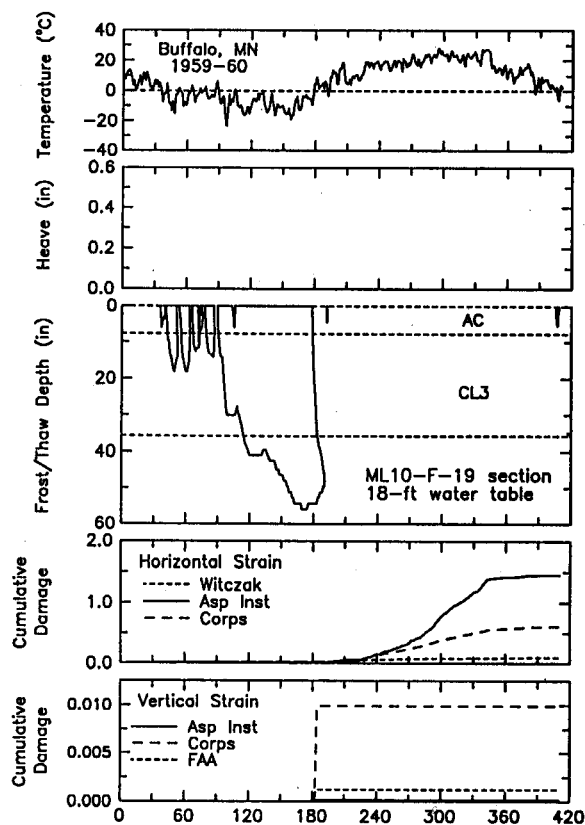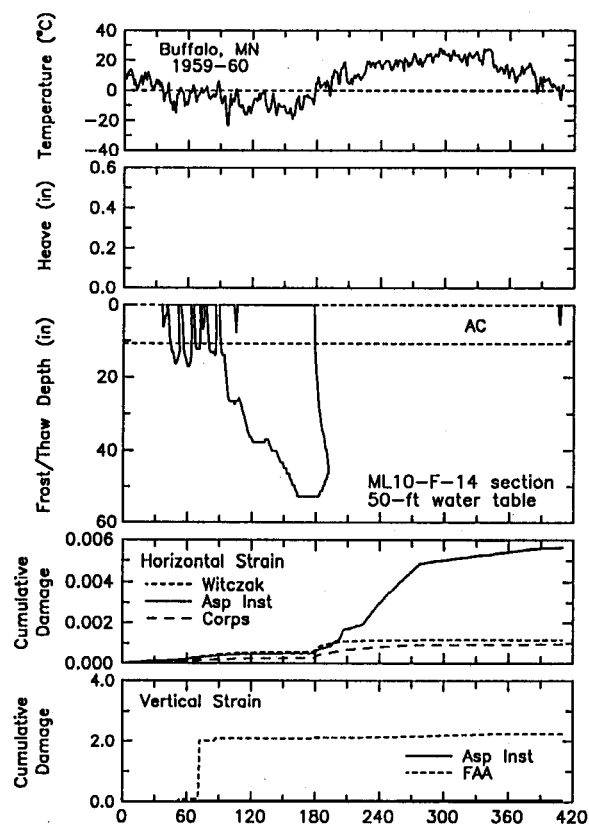

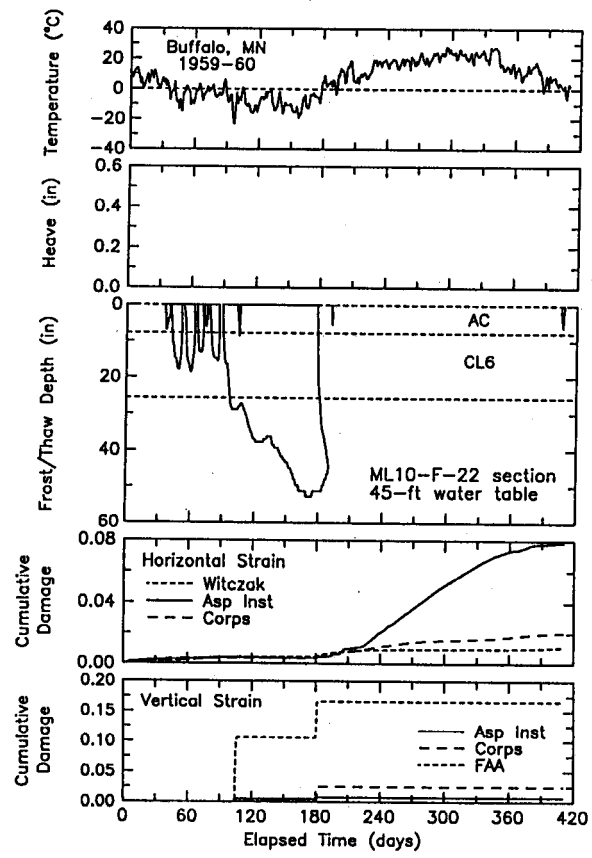* This was written by George Cochran, Mn/ROAD, pers. comm. 1994.

Irwin, L. and D. Speck (1986) NELAPAV user's guide. Cornell University, Ithaca, New York, Cornell University Local Road Program Report No. 86-1.

Mahoney, J.P., J.A. Lary, J. Sharma and N. Jackson (1985) Investigation of seasonal load restrictions in Washington state. Transportation Research Record 1043, Transportation Research Board, National Research Council, Washington D.C., p. 58–67.

Schmidt, R.J. (1975) Use of ASTM tests to predict low temperature stiffness of asphalt mixes. Transportation Research Record 544, Transportation Research Board, National Research Council, Washington, D.C. p. 35–45.

Ullidtz, P. (1987) *Pavement Analysis*. In *Developments in Civil Engineering*, Vol. 19, Amsterdam: Elsevier Science Publishers.

U.S. Army (1966) Calculation methods for determination of depths of freeze and thaw in soils. Department of the Army, Washington, D.C. Technical Manual TM 5-852-6.

U.S. Army (1987) Flexible pavement design for airfields (layered elastic method). Department of the Army, Washington, D.C. Technical Manual TM 5-825-2-1, Draft.

U.S. Army (1988) Pavement design for roads, streets, and open storage areas, elastic layered method. Department of the Army, Washington, D.C., Technical Manual TM 5-800-09.

U.S. Army (1990) Rigid pavements for airfields other than Army (layered elastic method). Department of the Army, Washington, D.C., Technical Manual TM 5-824-2-1.

Witczak, M. (1972) Design of full depth airfield pavements. In *Proceedings, Third International Conference on the Structural Design of Asphalt Pavements, London, England,* vol. I, p. 450–67.

Yang, W. (1988) Mechanistic analysis of nondestructive pavement deflection data. Doctorate Dissertation, Cornell University, Ithaca, New York (unpublished).

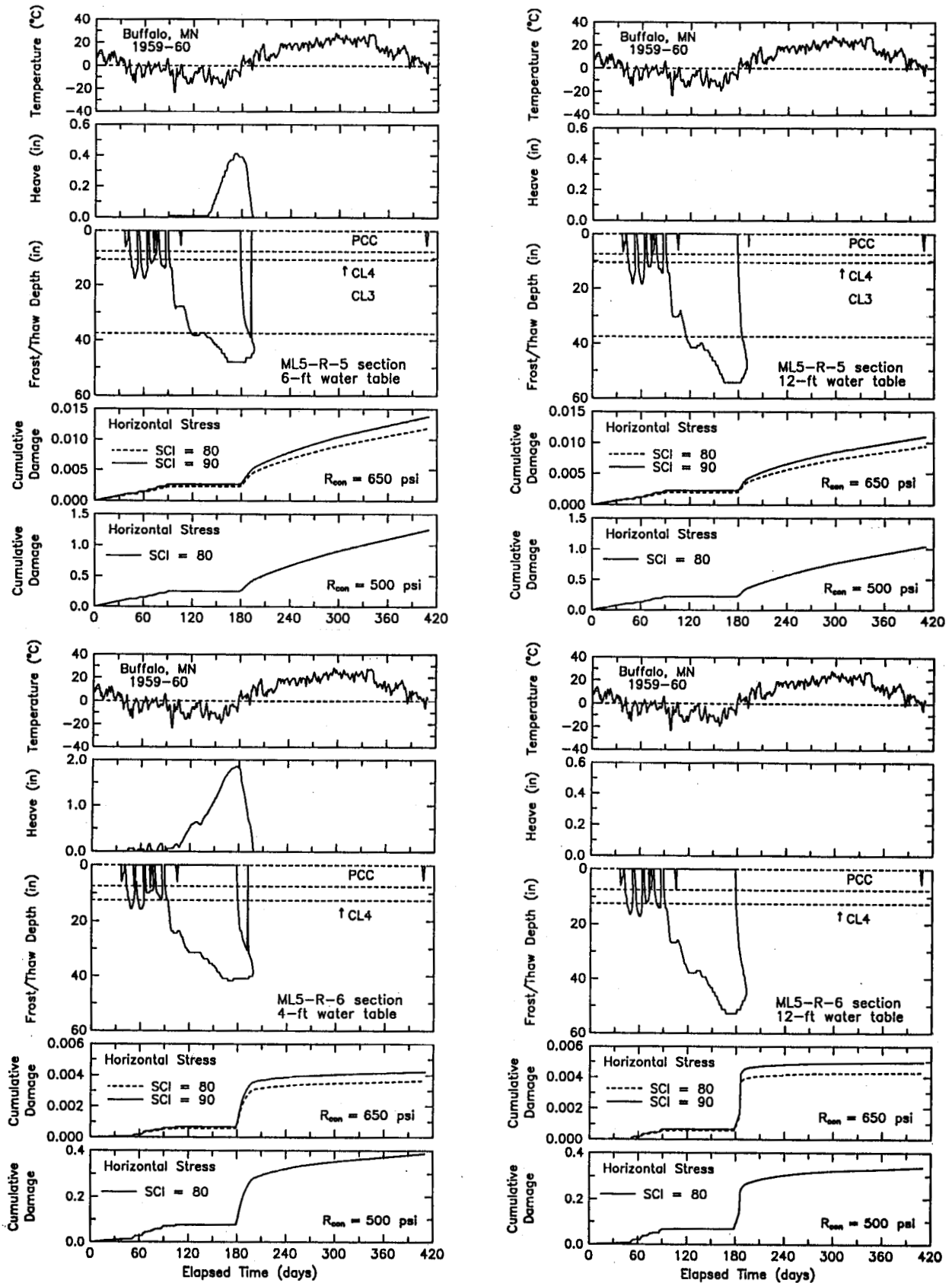APPENDIX B: HEAVE, FROST, AND CUMULATIVE DAMAGE OF RIGID SECTIONS

41

Left panel — Buffalo, MN 1959–60. Temperature (°C), Heave (in), Frost/Thaw Depth (in) with PCC and ↑CL4 lines, Cumulative Damage. ML10-R-11 section, 6-ft water table. Horizontal Stress, SCI = 80, R$_{con}$ = 500 psi.

Right panel — Buffalo, MN 1959–60. Temperature (°C), Heave (in), Frost/Thaw Depth (in) with PCC and ↑CL4 lines, Cumulative Damage. ML10-R-11 section, 12-ft water table. Horizontal Stress, SCI = 80, R$_{con}$ = 500 psi.

Elapsed Time (days)

REPORT DOCUMENTATION PAGE	*Form Approved* *OMB No. 0704-0188*

Public reporting burden for this collection of information is estimated to average 1 hour per response, including the time for reviewing instructions, searching existing data sources, gathering and maintaining the data needed, and completing and reviewing the collection of information. Send comments regarding this burden estimate or any other aspect of this collection of information, including suggestion for reducing this burden, to Washington Headquarters Services, Directorate for Information Operations and Reports, 1215 Jefferson Davis Highway, Suite 1204, Arlington, VA 22202-4302, and to the Office of Management and Budget, Paperwork Reduction Project (0704-0188), Washington, DC 20503.

1. AGENCY USE ONLY (Leave blank)	2. REPORT DATE September 1996	3. REPORT TYPE AND DATES COVERED Final Report May 1991–October 1994	
4. TITLE AND SUBTITLE Modeling of Mn/ROAD Test Sections with the CRREL Mechanistic Pavement Design Procedure		5. FUNDING NUMBERS CPAR Project Agreement No. 64632 Task Order No. 1	
6. AUTHORS Susan R. Bigl and Richard L. Berg			
7. PERFORMING ORGANIZATION NAME(S) AND ADDRESS(ES) U.S. Army Cold Regions Research and Engineering Laboratory 72 Lyme Road Hanover, New Hampshire 03755-1290		8. PERFORMING ORGANIZATION REPORT NUMBER Special Report 96-21	
9. SPONSORING/MONITORING AGENCY NAME(S) AND ADDRESS(ES) Minnesota Department of Transportation 395 John Ireland Boulevard Mail Stop 330 St. Paul, Minnesota 55155		10. SPONSORING/MONITORING AGENCY REPORT NUMBER MN/RC-96/22	
11. SUPPLEMENTARY NOTES For conversion of SI units to non-SI units of measurement consult ASTM Standard E380-93, *Standard Practice for Use of the International System of Units,* published by the American Society for Testing and Materials, 1916 Race St., Philadelphia, Pa. 19103.			
12a. DISTRIBUTION/AVAILABILITY STATEMENT Approved for public release; distribution is unlimited. Available from NTIS, Springfield, Virginia 22161		12b. DISTRIBUTION CODE	

13. ABSTRACT (*Maximum 200 words*)

The U.S. Army Cold Regions Research and Engineering Laboratory is developing a mechanistic pavement design procedure for use in seasonal frost areas. The procedure was used to predict pavement performance of some test sections at the Mn/ROAD facility. Simulations were conducted in three phases, investigating the effects on predictions of water table position, subgrade characteristics, asphalt model, and freeze season characteristics. The procedure predicted significantly different performance by the different test sections and highly variable results depending on the performance model applied. The simulated performance of the tests sections also was greatly affected by the subgrade conditions, e.g., density, soil moisture, and water table depth. In general, predictions for the full-depth asphalt sections indicate that they will not fail due to cracking, but two of the three criteria for subgrade rutting indicate failure before the five- or 10-year design life of the sections. Conventional sections are predicted not to fail due to subgrade rutting; however, sections including the more frost-susceptible bases in their design are predicted to fail due to asphalt cracking relatively early in their design life, and sections with non-frost-susceptible bases are predicted to fail towards the end of the design life.

14. SUBJECT TERMS			15. NUMBER OF PAGES 51
Freeze season characteristics Mechanistic Pavement Design and Evaluation Procedure		Pavement performance	16. PRICE CODE

17. SECURITY CLASSIFICATION OF REPORT UNCLASSIFIED	18. SECURITY CLASSIFICATION OF THIS PAGE UNCLASSIFIED	19. SECURITY CLASSIFICATION OF ABSTRACT UNCLASSIFIED	20. LIMITATION OF ABSTRACT UL

NSN 7540-01-280-5500

Standard Form 298 (Rev. 2-89)
Prescribed by ANSI Std. Z39-18
298-102